Supporting Information

Development of two fluorescent chemosensors for selective detection of Zn^{2+} and Al^{3+} ions in quinoline platform by tuning of substituent in the receptor part: Elucidation of structures of metal bound chemosensors and biological studies

Pravat Ghorai,[a] Kunal Pal,[b] Parimal Karmakar,[b] and Amrita Saha*[a]

[a]*Department of Chemistry, Jadavpur University, Kolkata- 700032, India.*

E-mail: amritasahachemju@gmail.com; Tel. +91-33-24572941

[b]*Department of Life Science and Biotechnology, Jadavpur University, Kolkata-700032, India.*

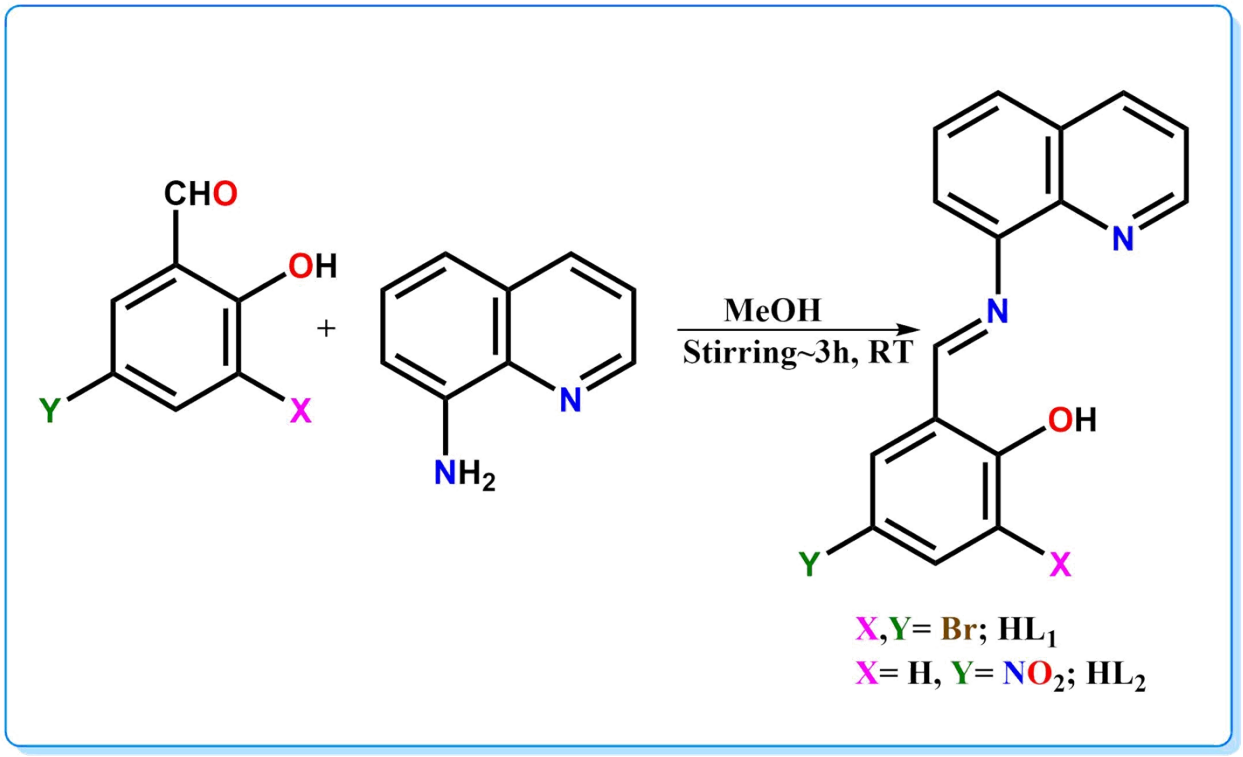

Scheme S1 Route to the synthesis of chemosensors (**HL_1** and **HL_2**).

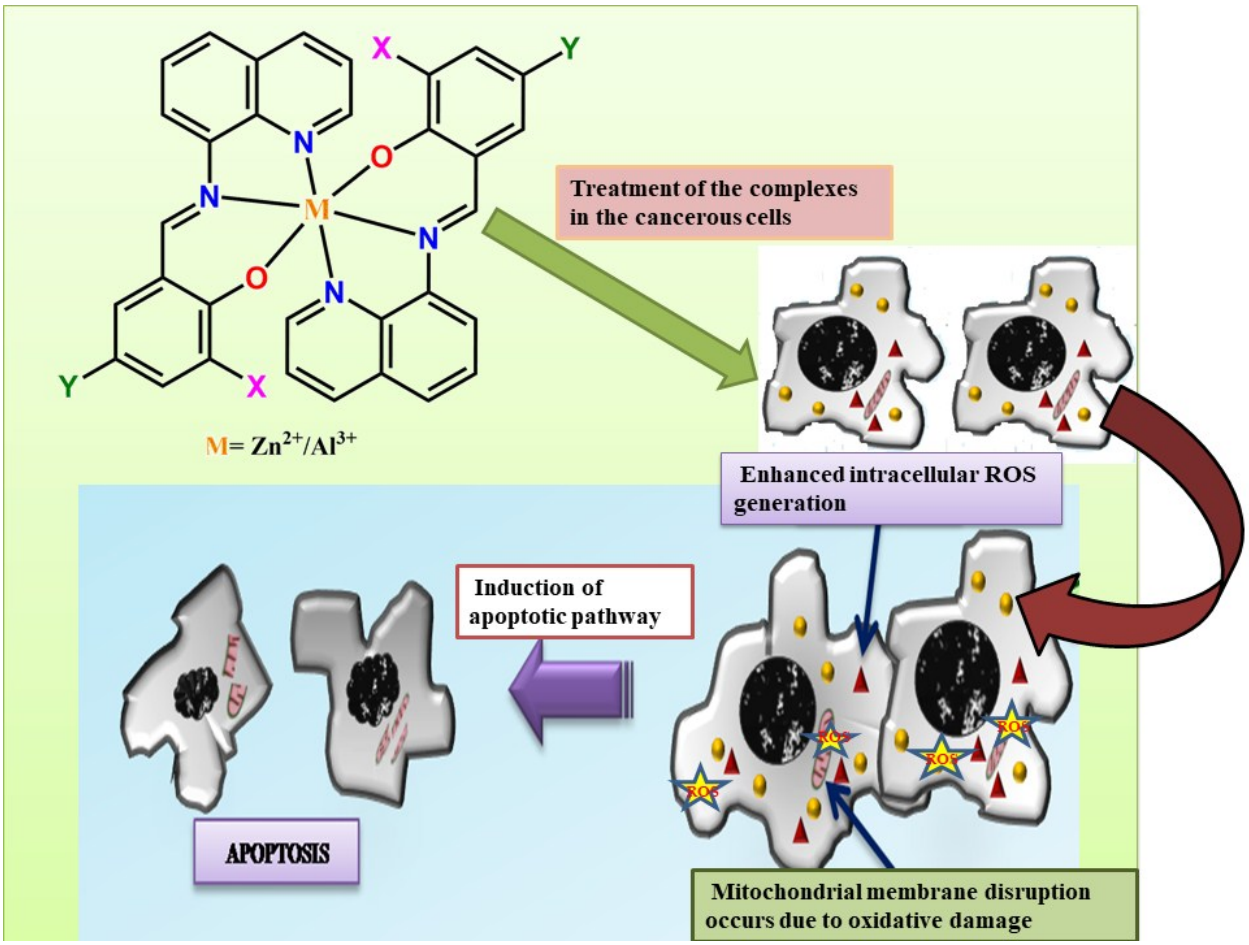

Scheme S2 Enhancement of ROS in presence of complexes **1** and **2**.

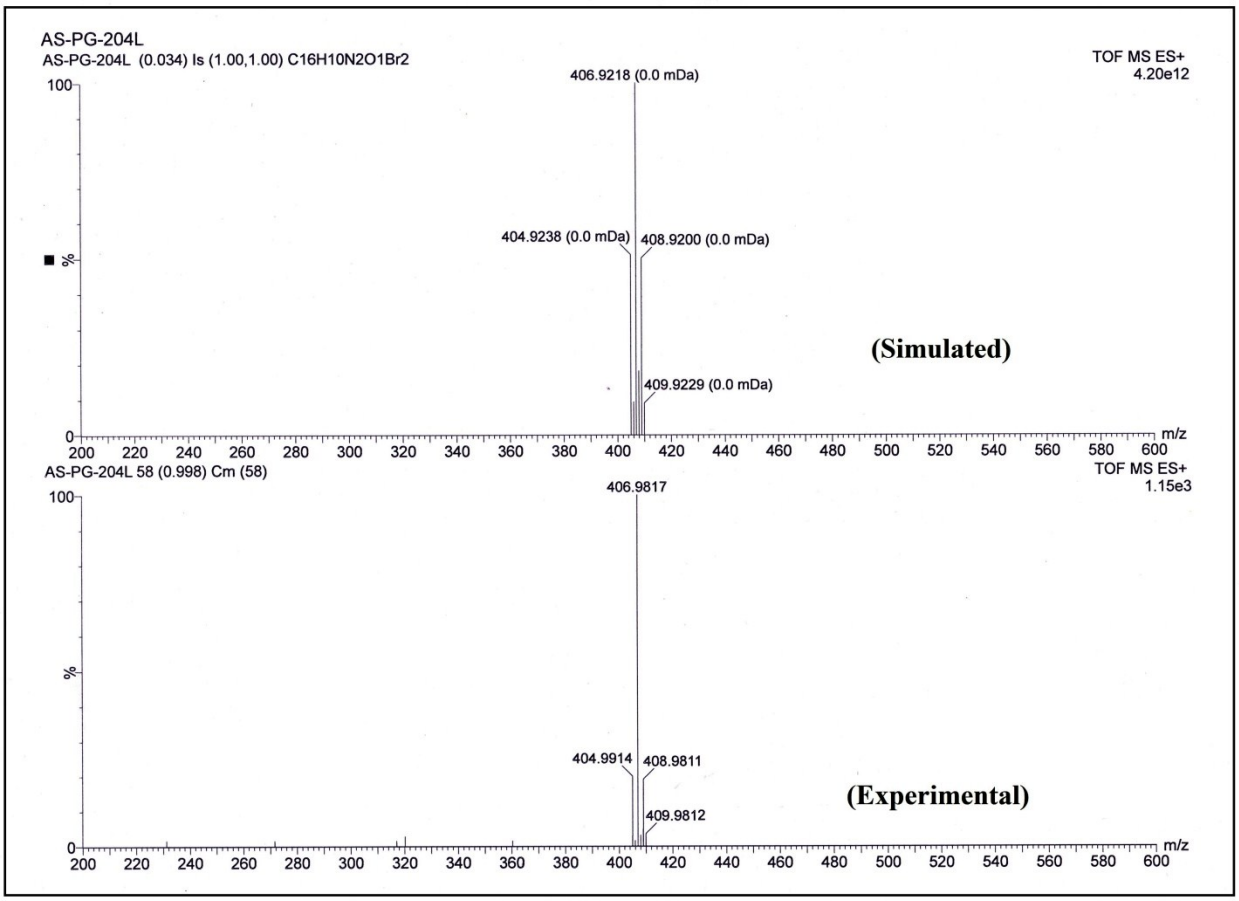

Fig. S1 ESI-MS spectrum of $\mathbf{HL_1}$.

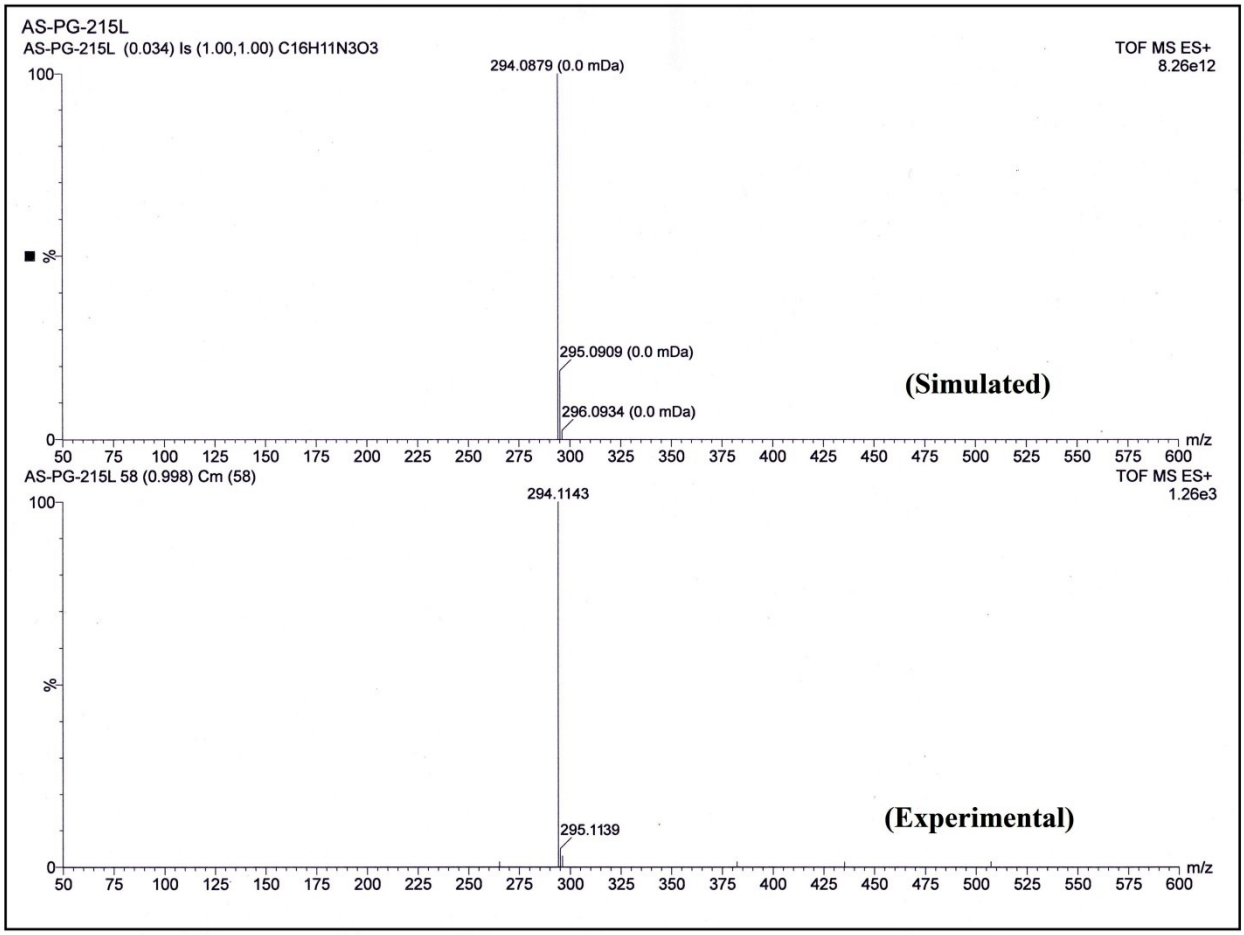

Fig. S2 ESI-MS spectrum of $\mathbf{HL_2}$.

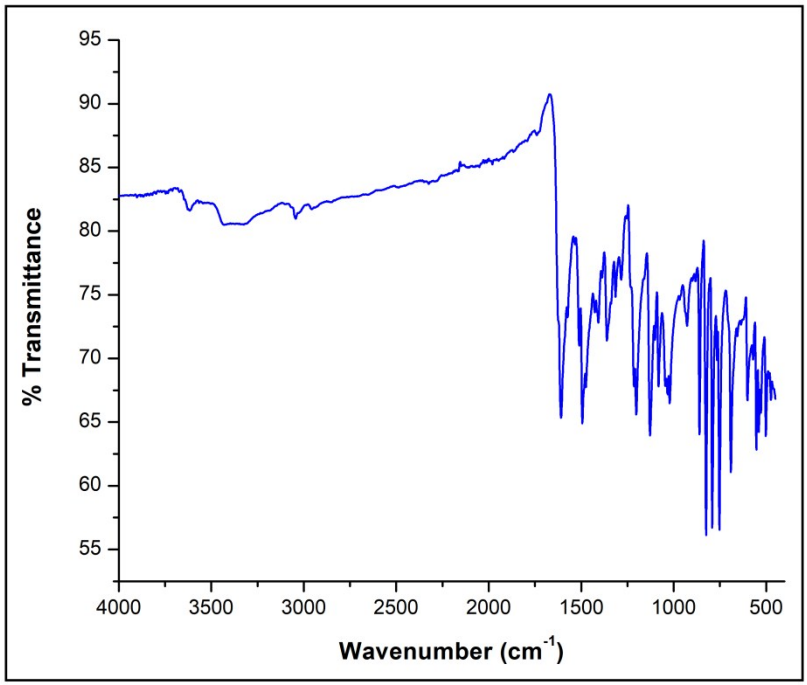

Fig. S3 FT-IR spectrum of $\mathbf{HL_1}$.

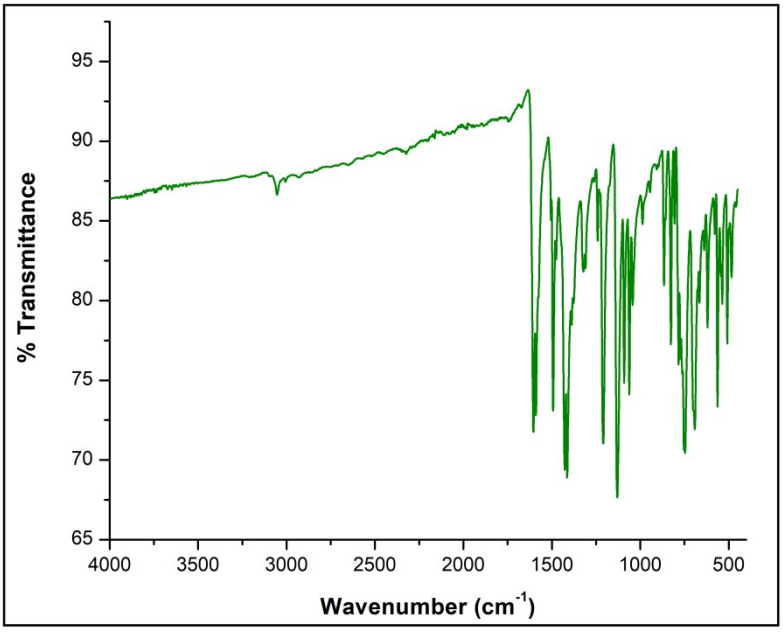

Fig. S4 FT-IR spectrum of $\mathbf{HL_2}$.

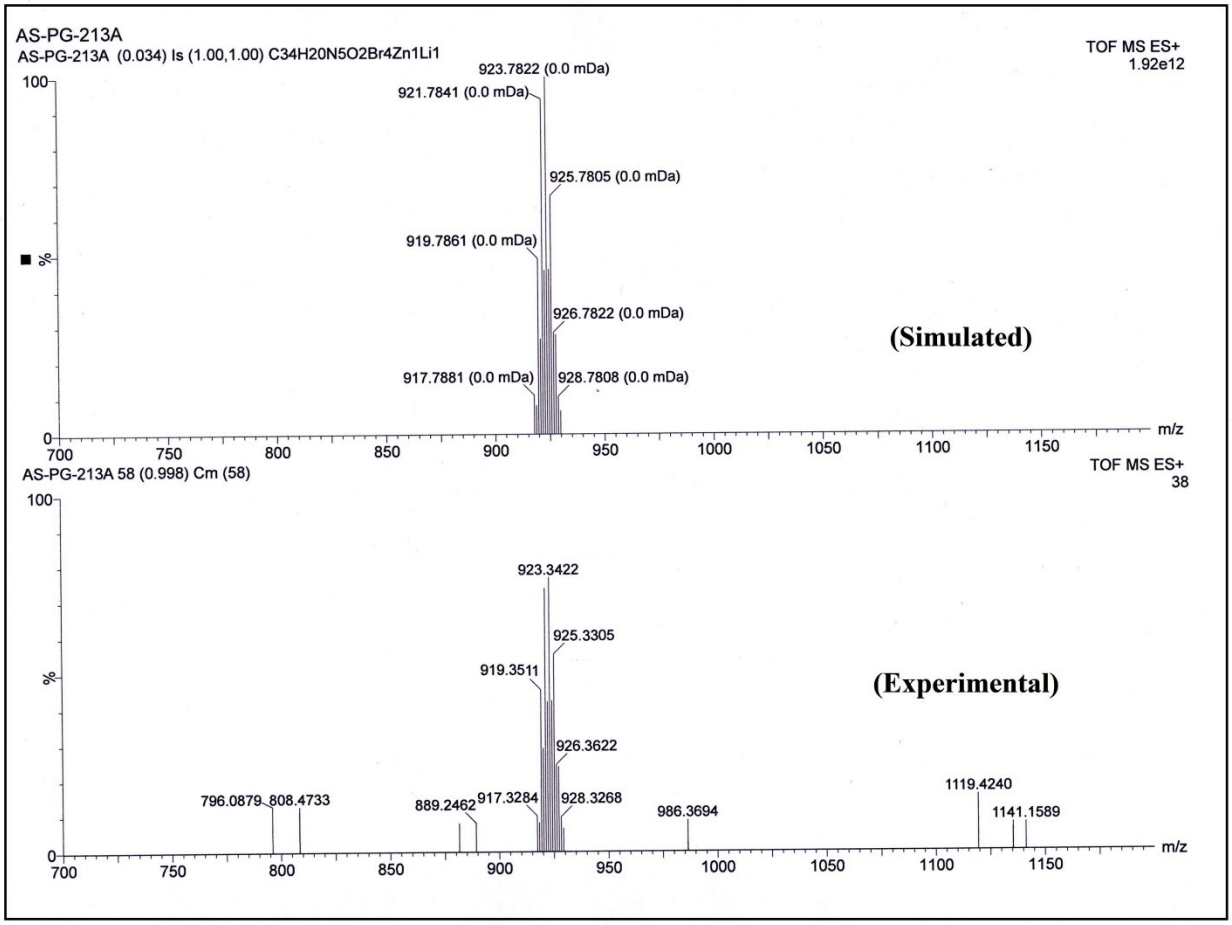

Fig. S5 ESI-MS spectrum of complex **1**.

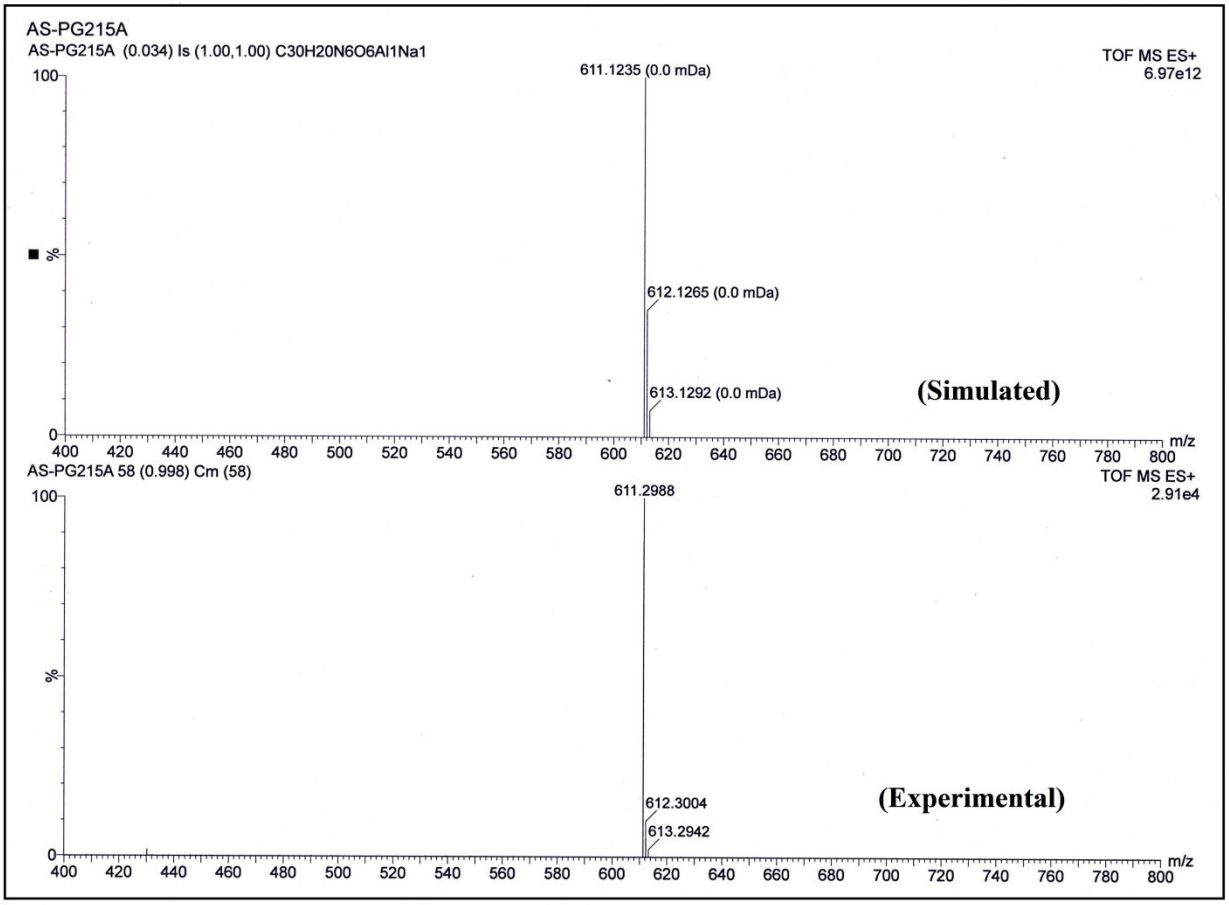

Fig. S6 ESI-MS spectrum of complex **2**.

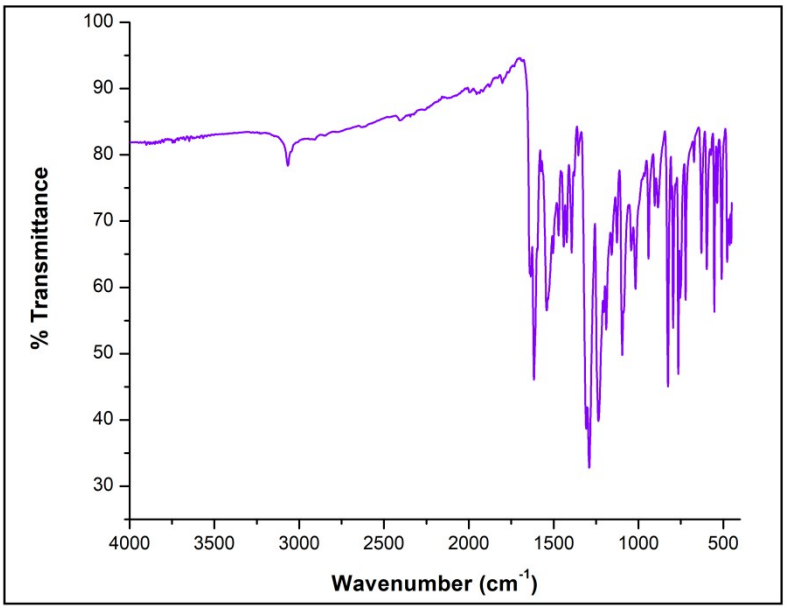

Fig. S7 FT-IR spectrum of complex **1**.

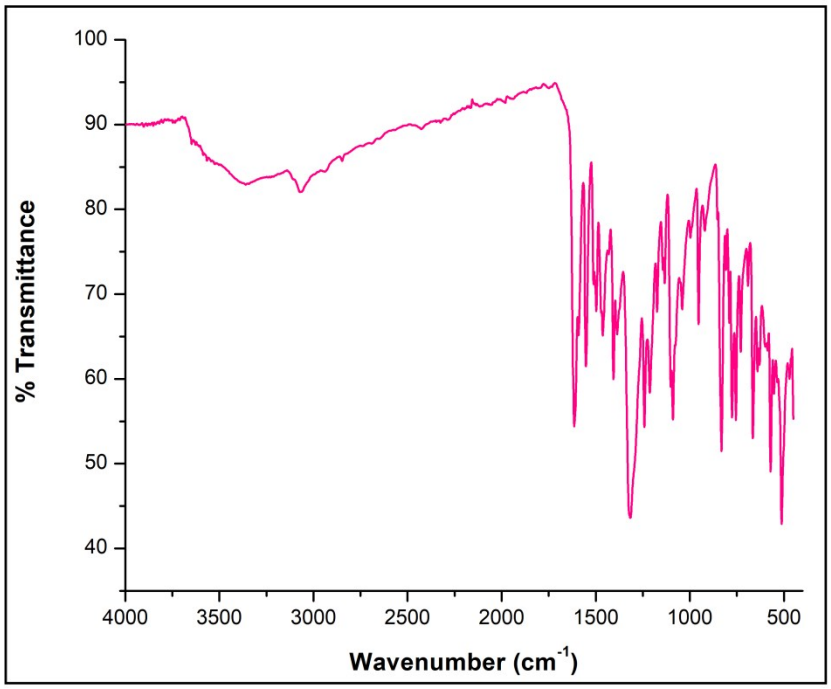

Fig. S8 FT-IR spectrum of complex **2**.

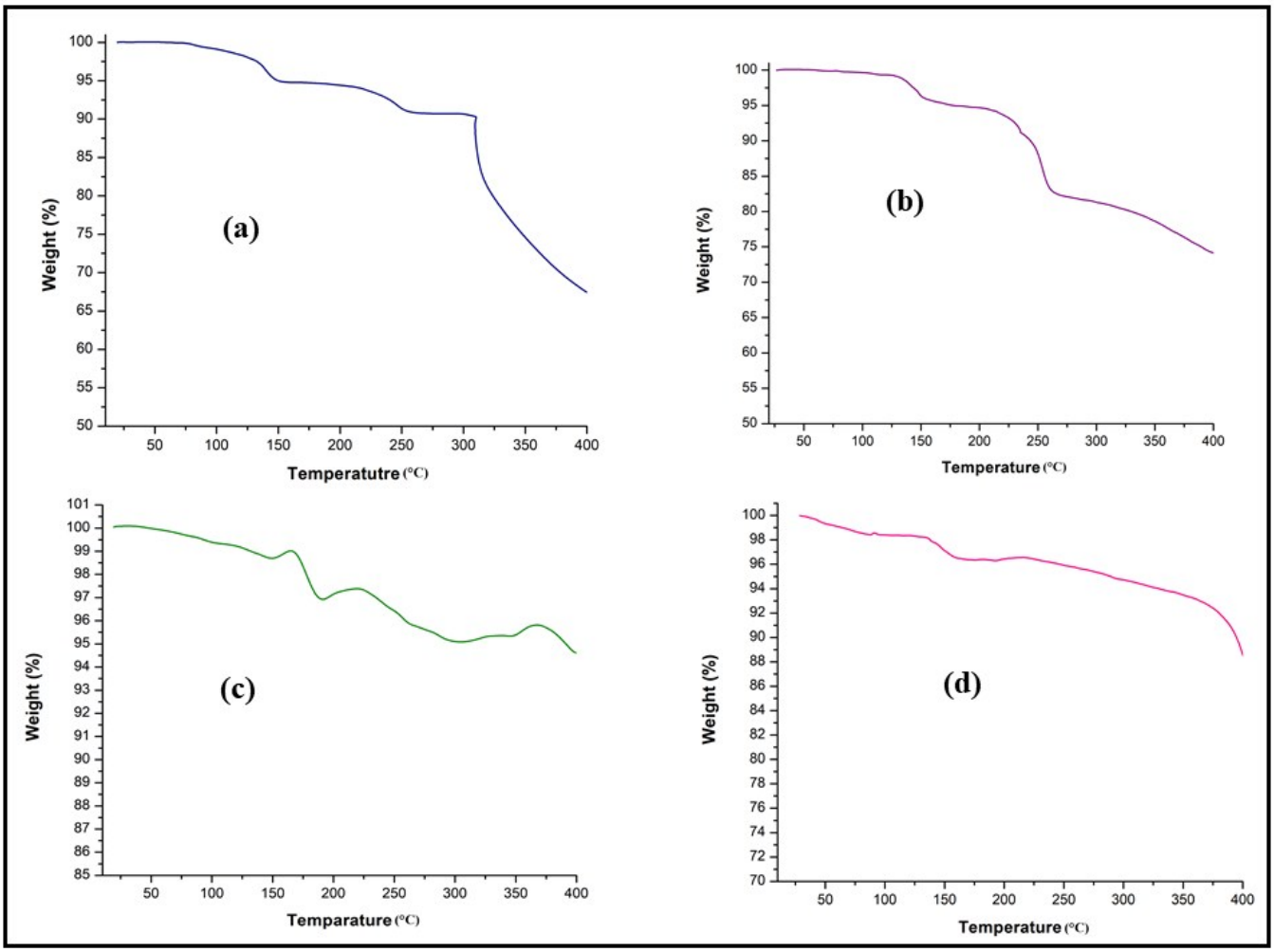

Fig. S9 Thermo Gravimetric Analysis of (a) $\mathbf{HL_1}$, (b) $\mathbf{HL_2}$, (c) complex **1** and (d) complex **2** under nitrogen atmosphere.

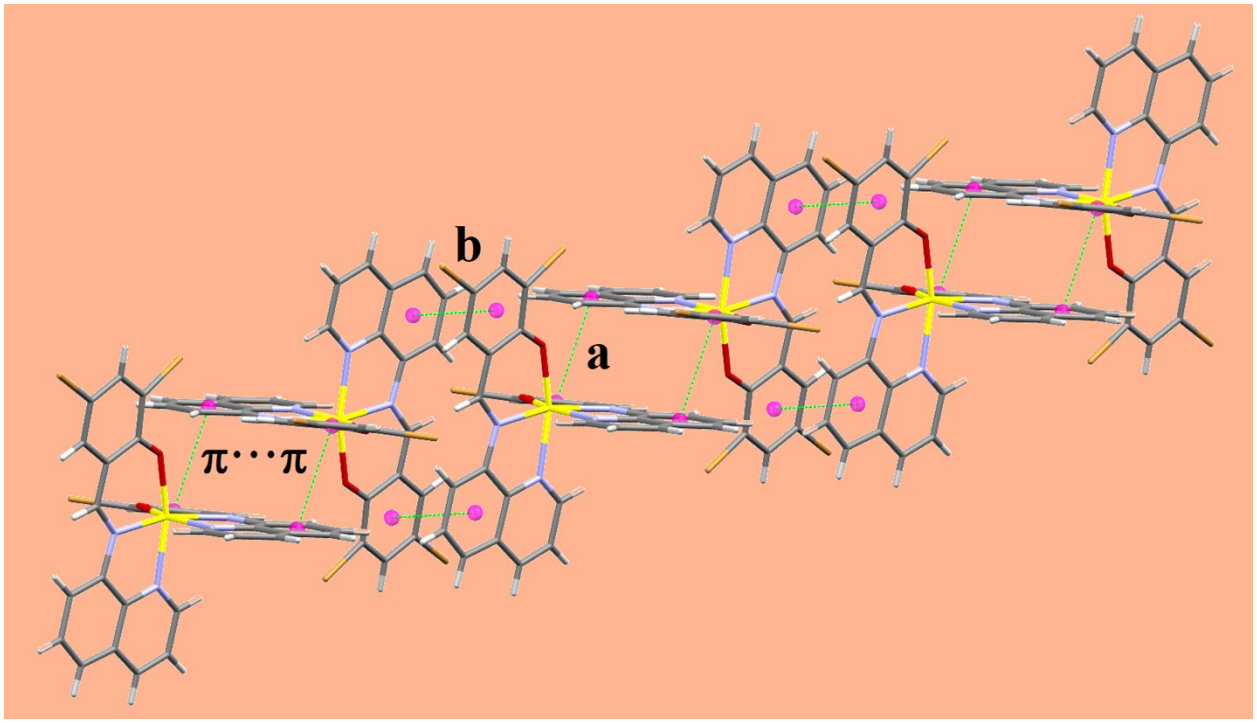

Fig. S10a π···π interactions of complex **1** along the ab plane (a= 3.484Å and b=3.512 Å).

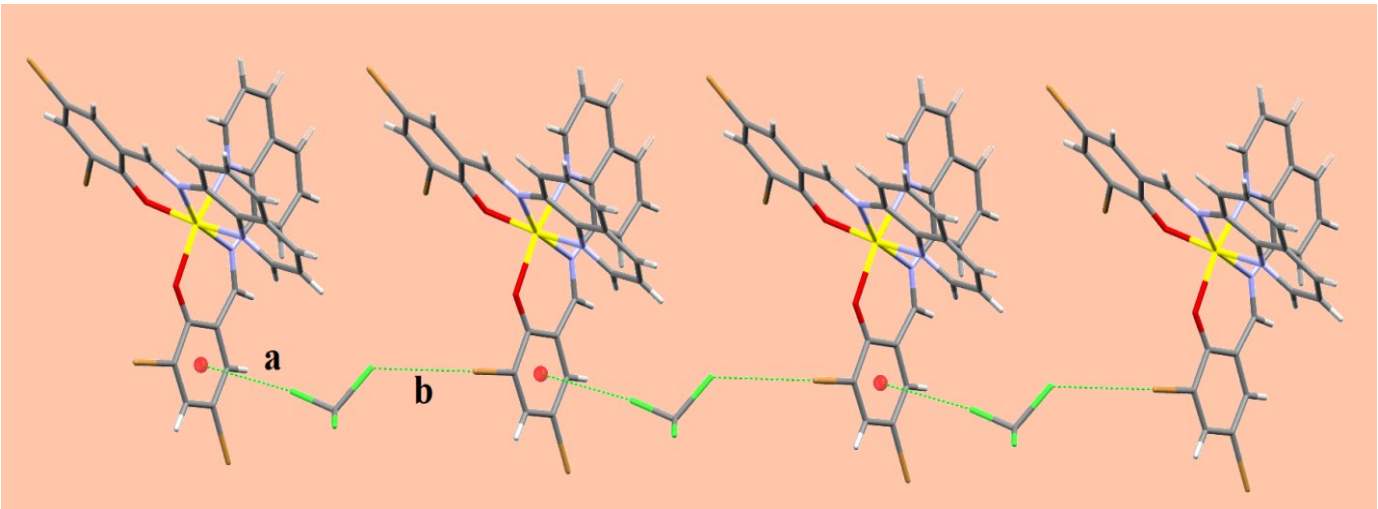

Fig. S10b Halogen···π and halogen···halogen interactions of complex **1** along the a axis (a= 3.525Å and b=3.639Å).

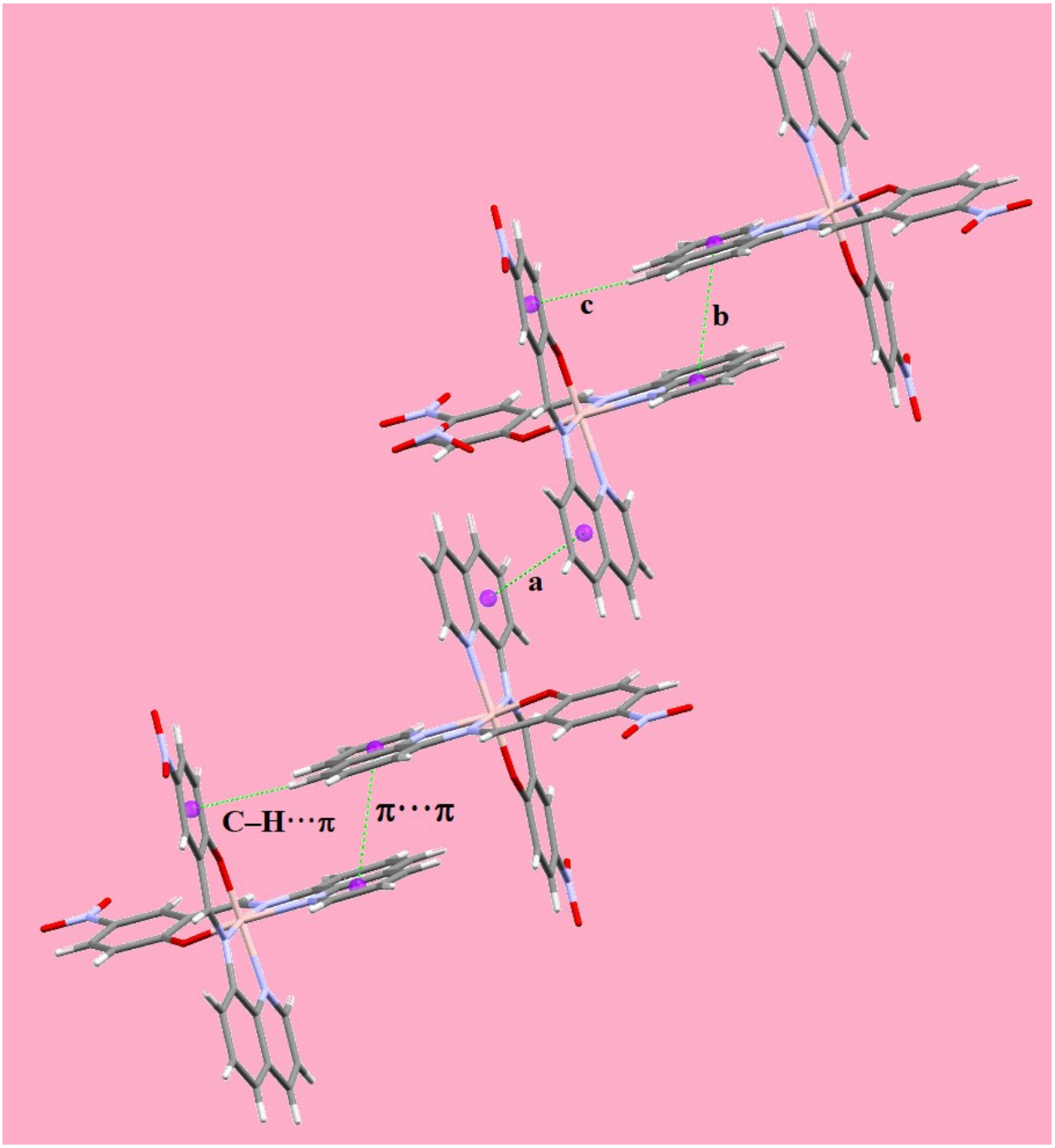

Fig. S11 Different supramolecular interactions of complex **2** along the c axis (a= 3.569Å; b=3.842 Å and c= 2.909Å).

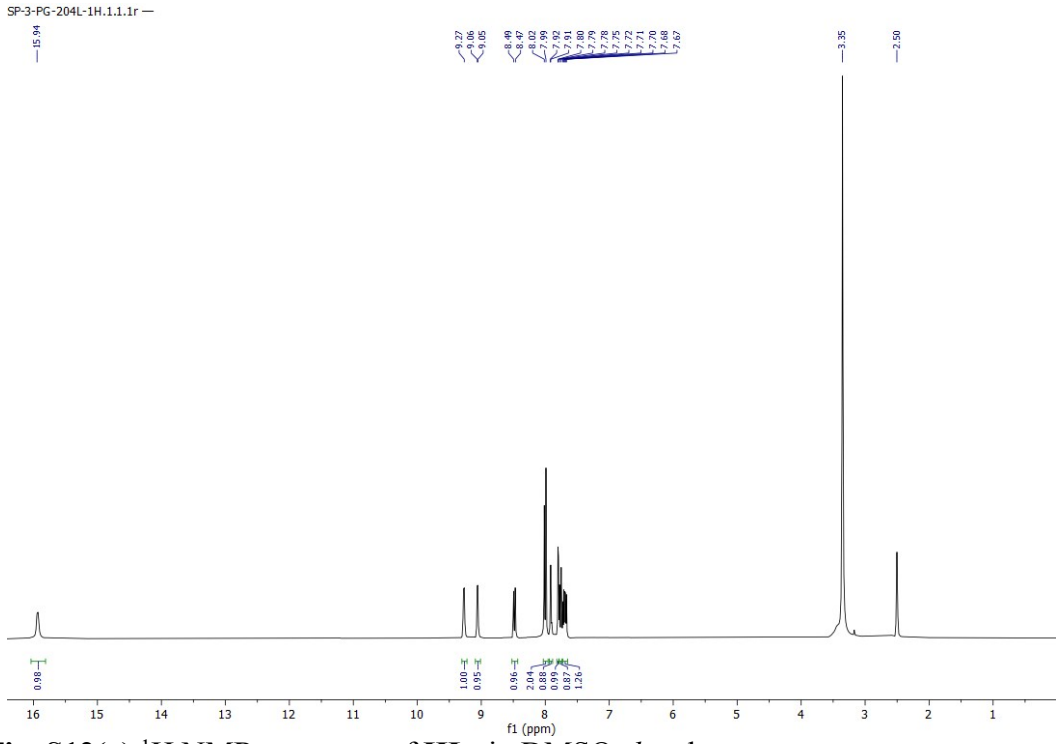

Fig. S12(a) ^{1}H NMR spectrum of $\mathbf{HL_1}$ in DMSO-d_6 solvent.

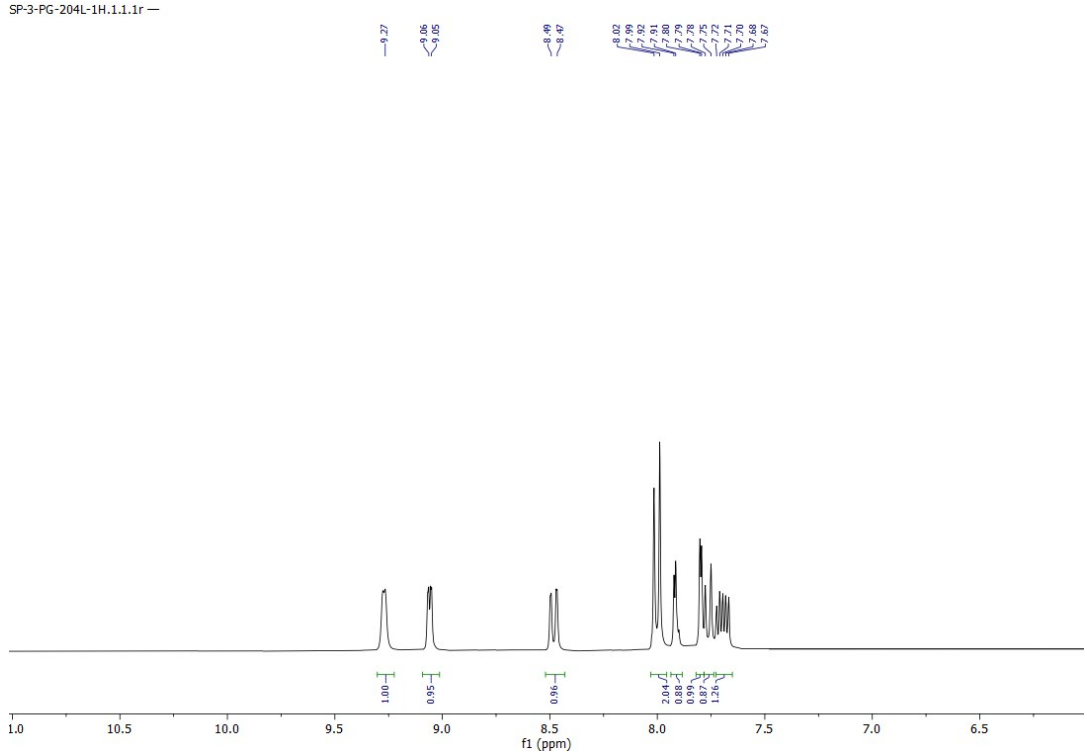

Fig. S12(b) Expanded view of ^{1}H NMR spectrum of $\mathbf{HL_1}$ in DMSO-d_6 solvent.

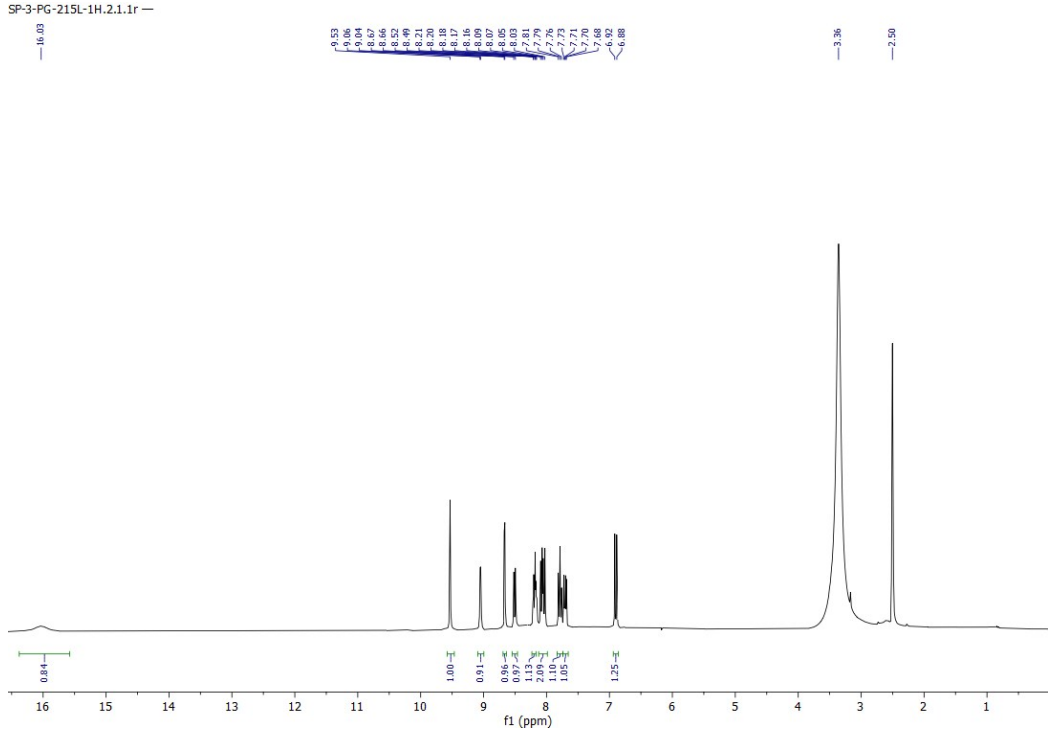

Fig. S13(a) ^{1}H NMR spectrum of **HL$_2$** in DMSO-d_6 solvent.

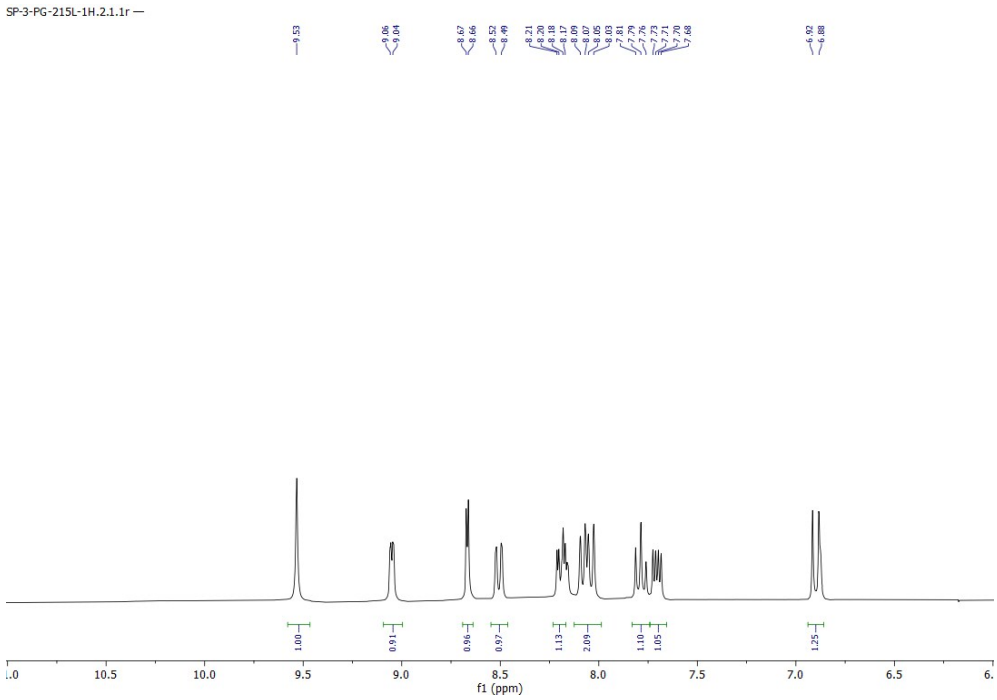

Fig. S13(b) Expanded view of ^{1}H NMR spectrum of **HL$_2$** in DMSO-d_6 solvent.

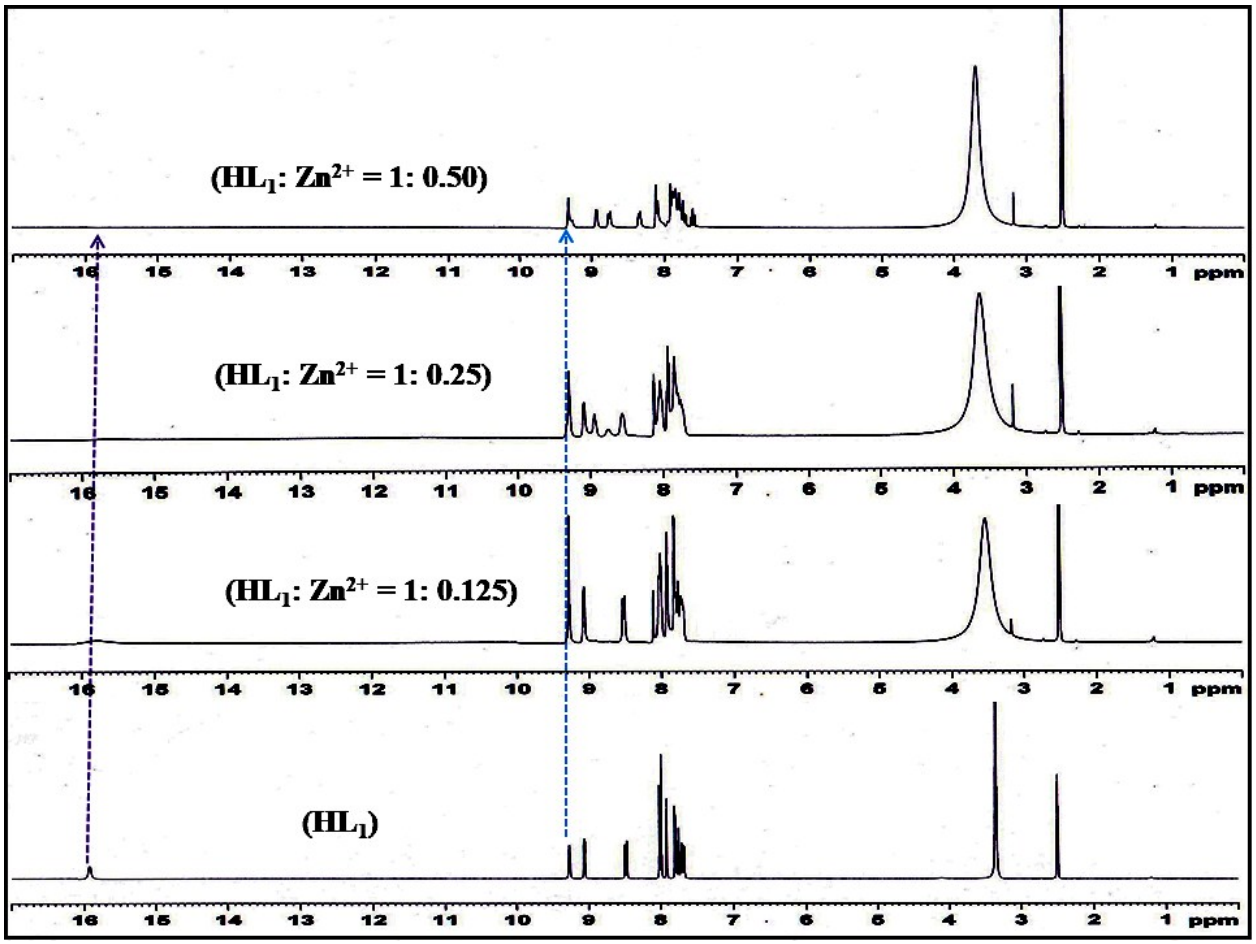

Fig. S14(a) ^{1}H-NMR spectrum of the free ligand **HL$_1$** and with the addition of 0.125, 0.25 and 0.50 equivalent of Zn^{2+} ion in DMSO-d_6 solvent.

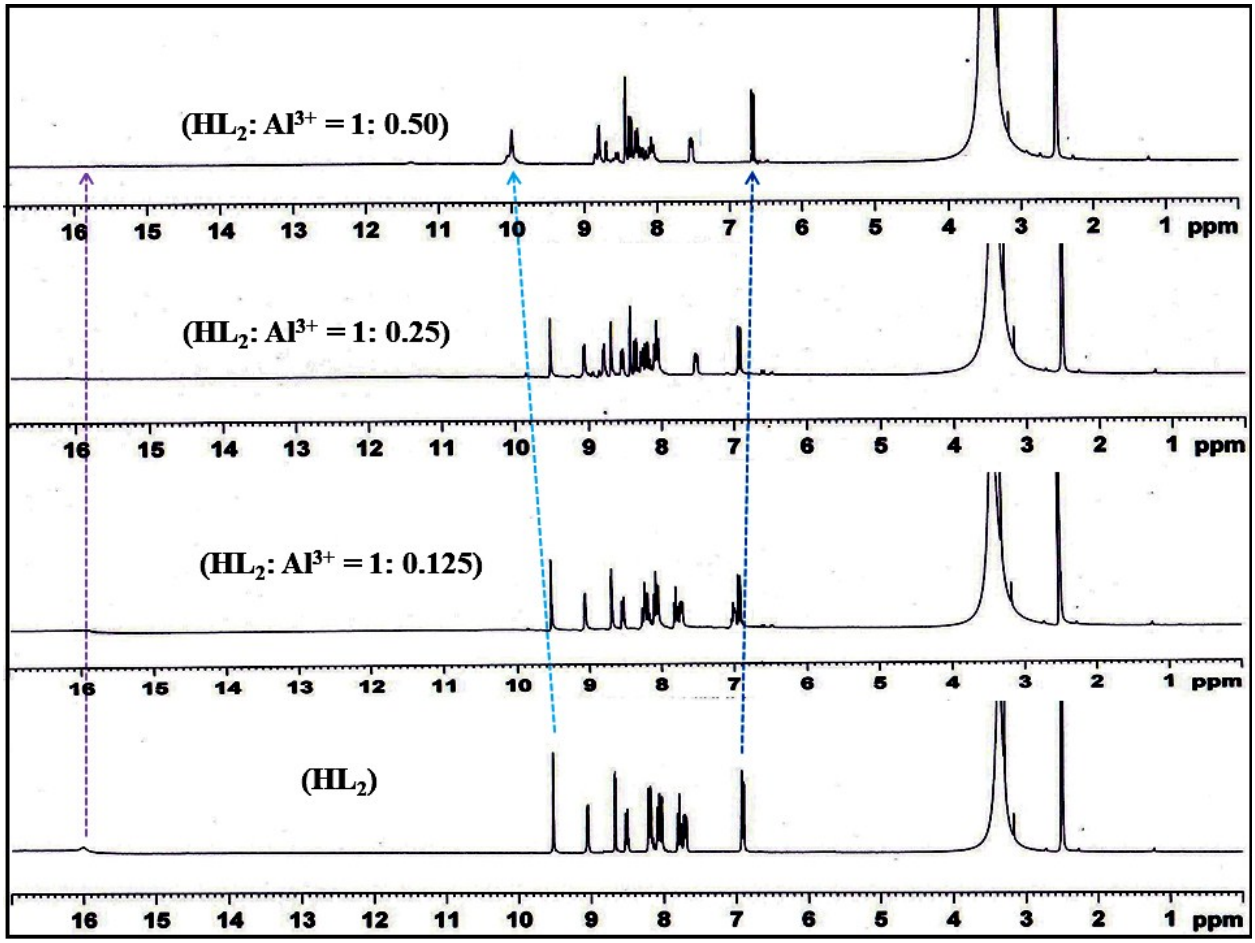

Fig. S14(b) ^{1}H-NMR spectrum of the free ligand **HL_2** and with the addition of 0.125, 0.25 and 0.50 equivalent of Al^{3+} ion in DMSO-d_6 solvent.

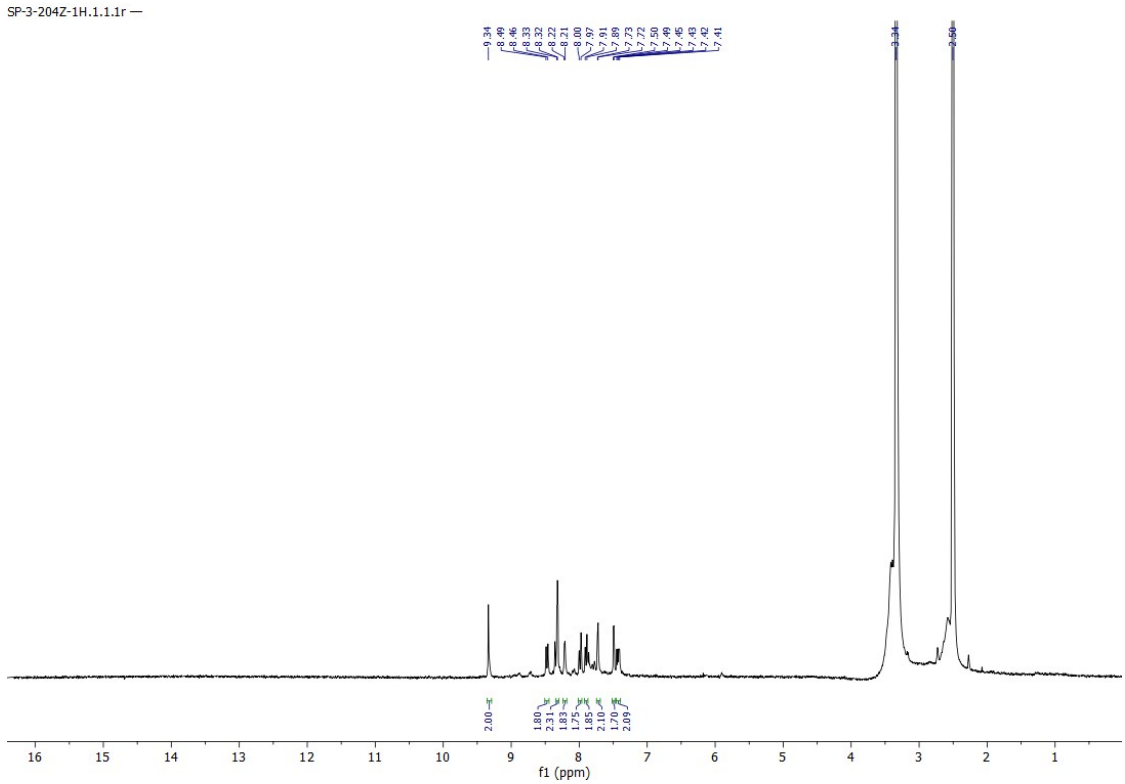

Fig. S15(a) ^{1}H NMR spectrum of complex **1** in DMSO-d_6 solvent.

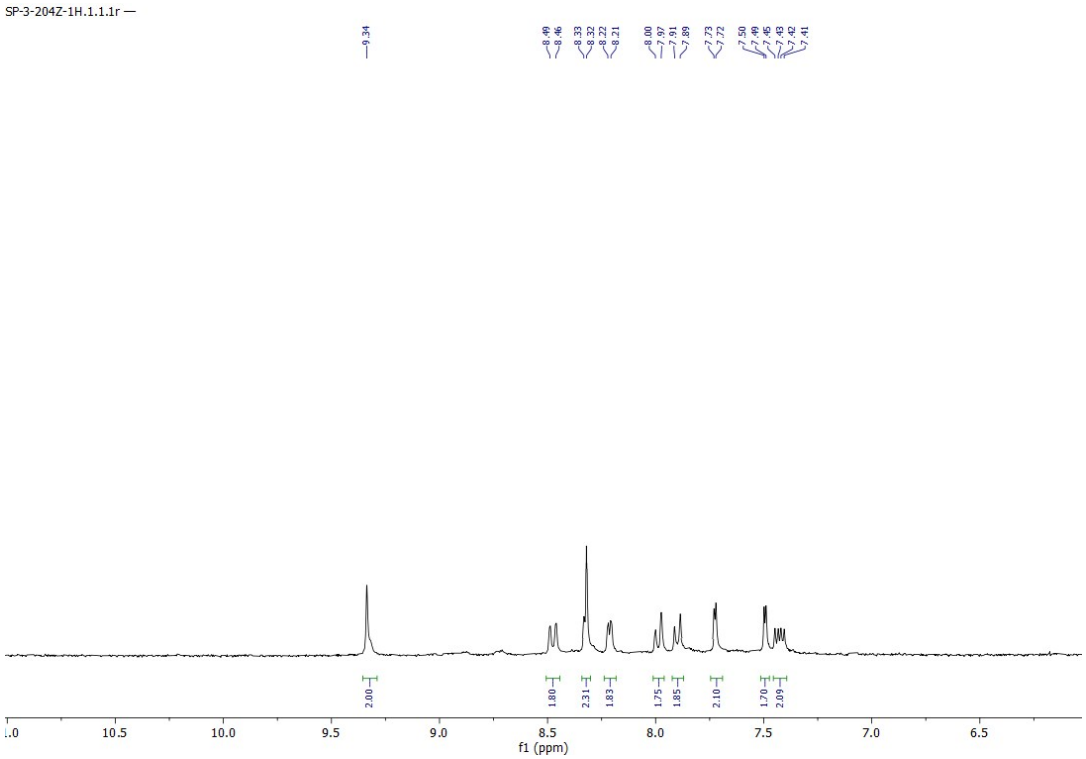

Fig. S15(b) Expanded view of ^{1}H NMR spectrum of complex **1** in DMSO-d_6 solvent.

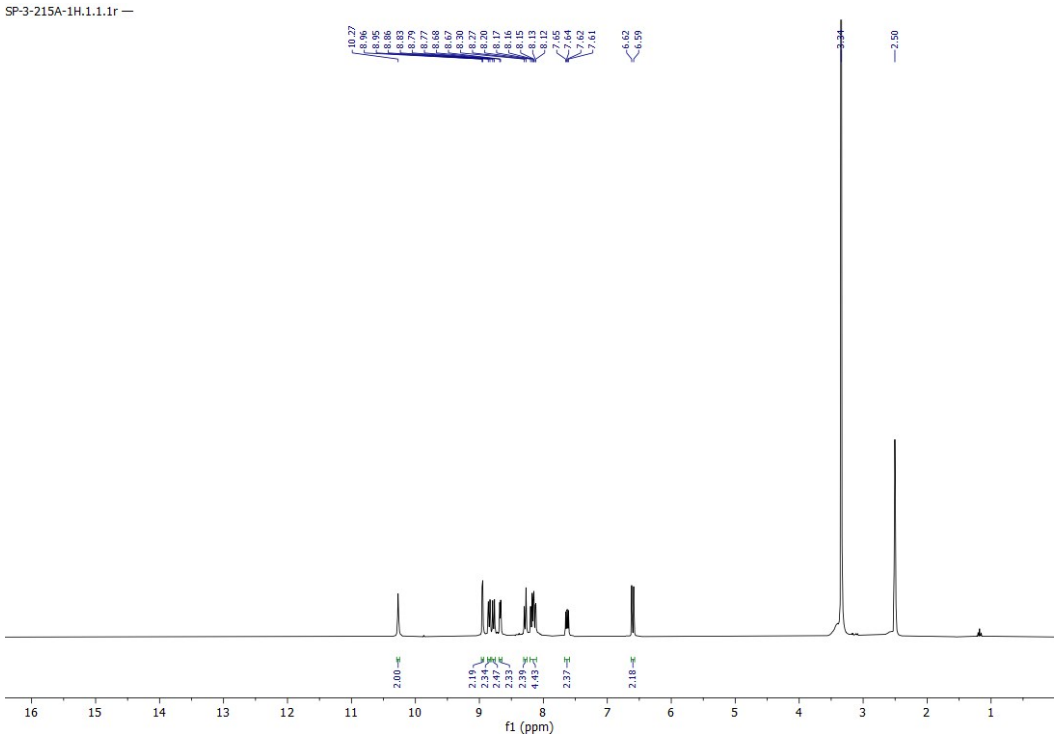

Fig. S16(a) ^{1}H NMR spectrum of complex **2** in DMSO-d_6 solvent.

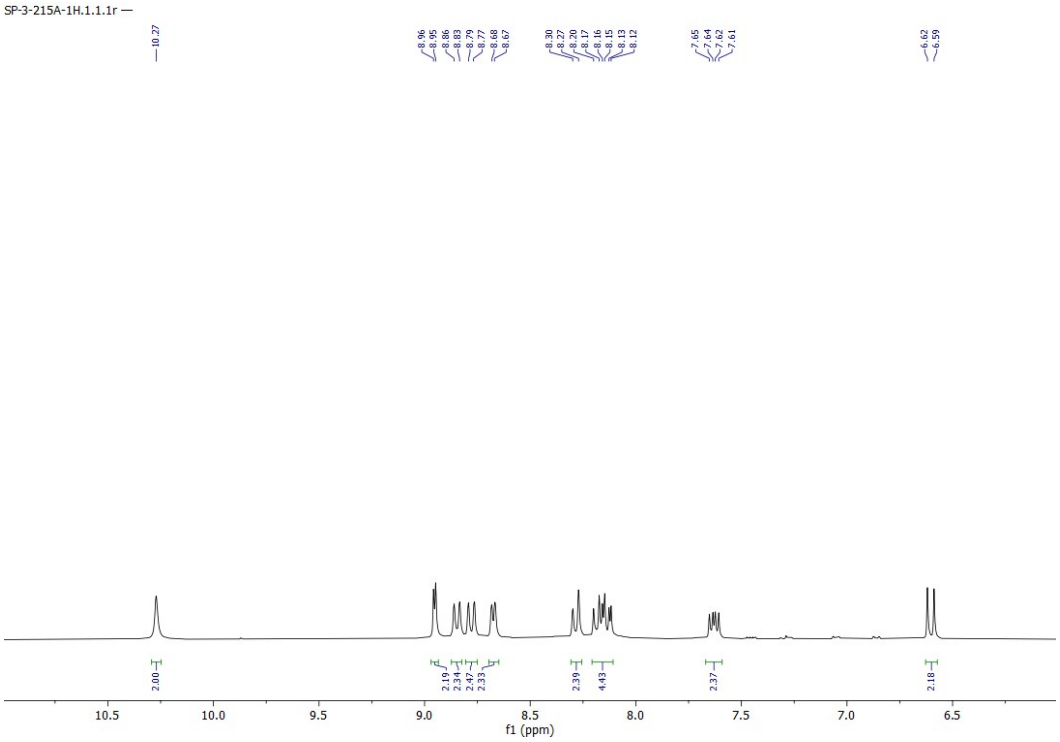

Fig. S16(b) Expanded view of ^{1}H NMR spectrum of complex **2** in DMSO-d_6 solvent.

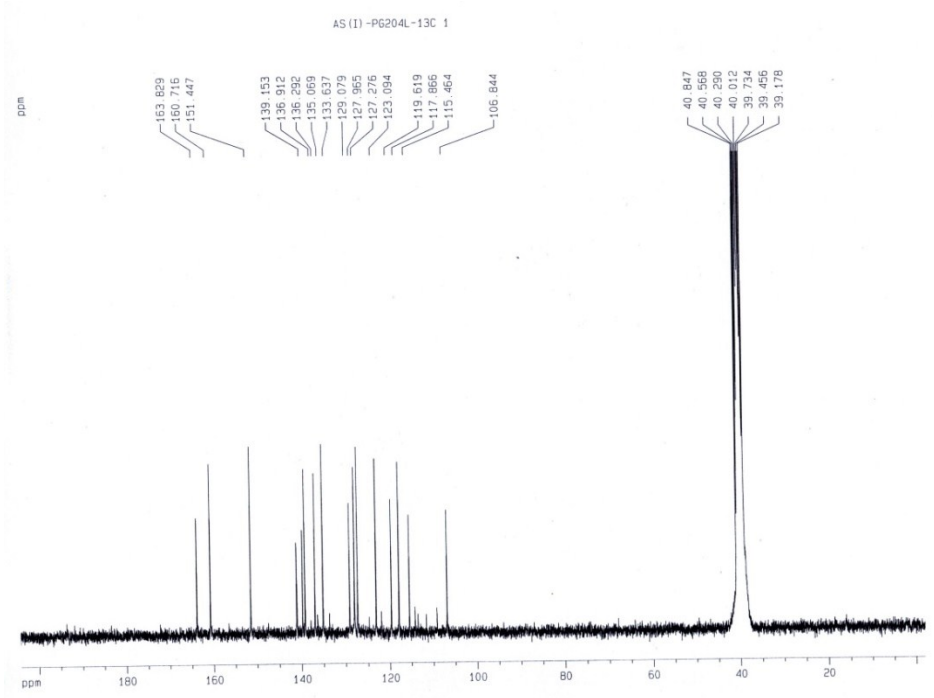

Fig. S17 ^{13}C NMR spectrum of **HL$_1$** in DMSO-d_6 solvent.

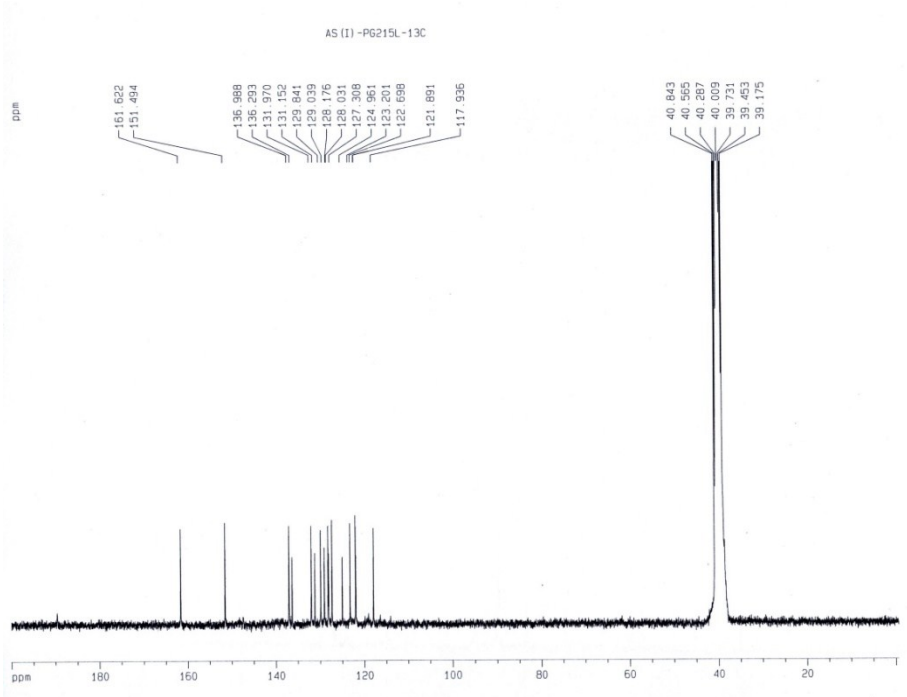

Fig. S18 ^{13}C NMR spectrum of **HL$_2$** in DMSO-d_6 solvent.

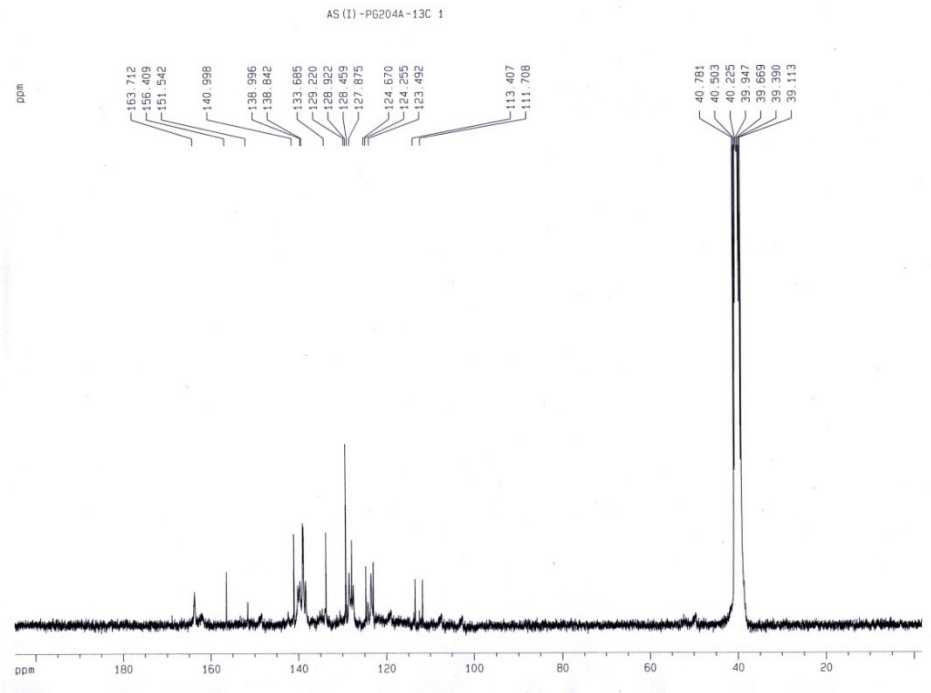

Fig. S19 ^{13}C NMR spectrum of complex **1** in DMSO-d_6 solvent.

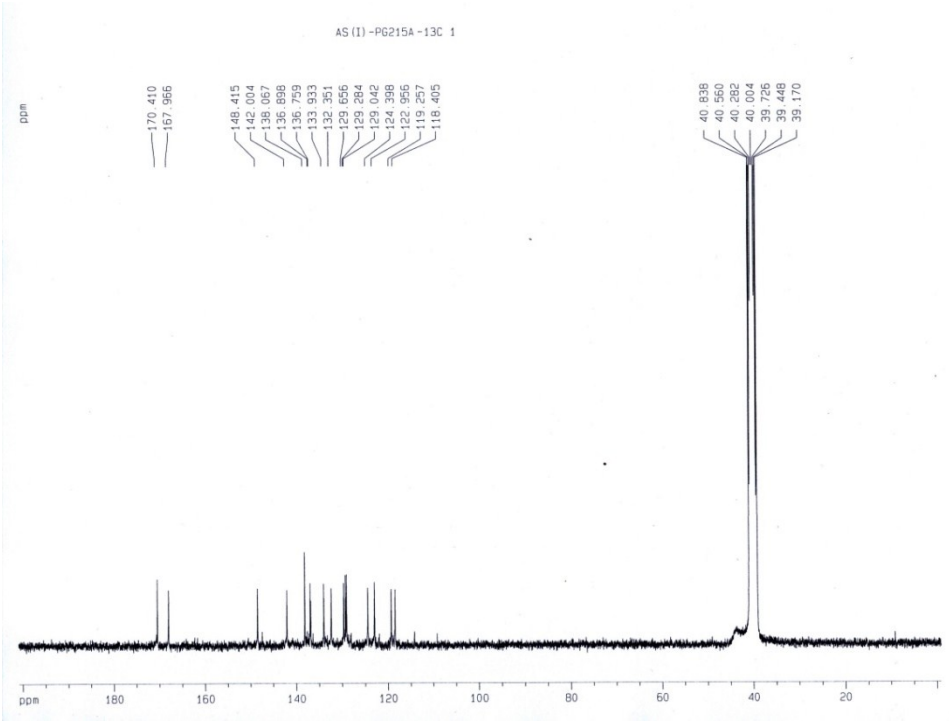

Fig. S20 ^{13}C NMR spectrum of complex **2** in DMSO-d_6 solvent.

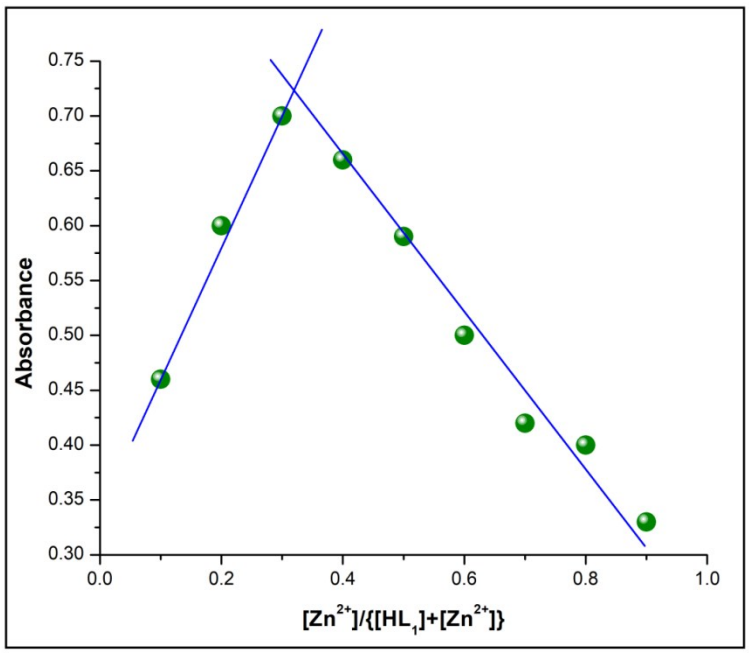

Fig. S21 1:2 binding stoichiometry of Zn^{2+} ions to the probe $\mathbf{HL_1}$, shown by Job's plot. Symbols and solid lines represent the experimental and simulated profiles, respectively.

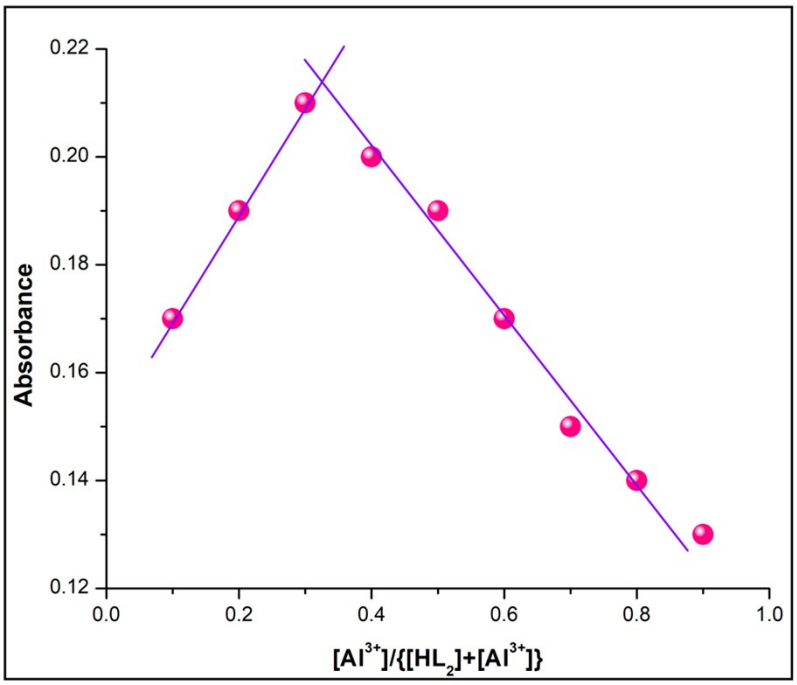

Fig. S22 1:2 binding stoichiometry of Al^{3+} ions to the probe $\mathbf{HL_2}$, shown by Job's plot. Symbols and solid lines represent the experimental and simulated profiles, respectively.

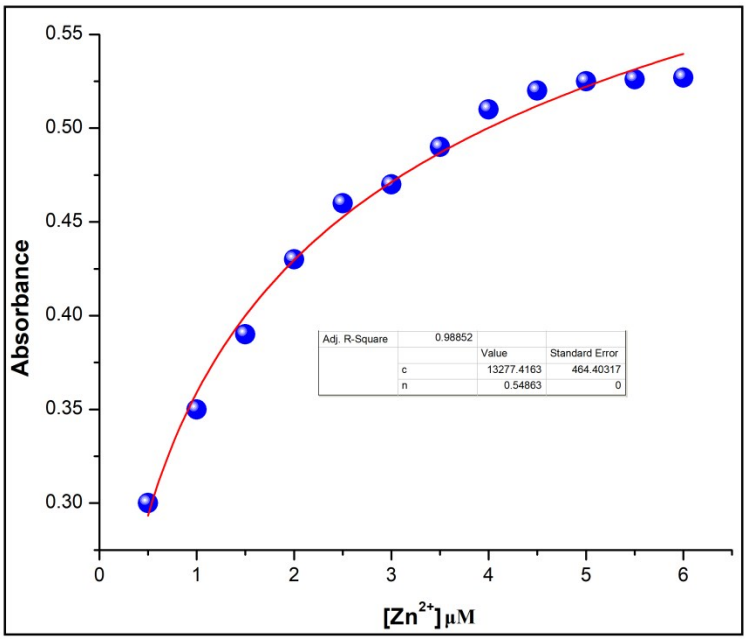

Fig. S23 Non-linear least square curve fitting for complex **1** by using UV-Vis titration plot of **HL_1** in presence of Zn^{2+} ions.

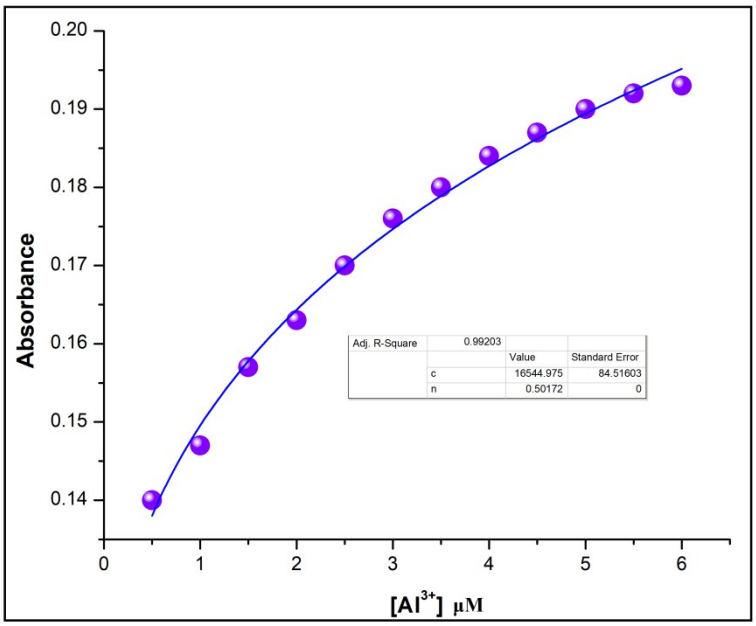

Fig. S24 Non-linear least square curve fitting for complex **2** by using UV-Vis titration plot of **HL_2** in presence of Al^{3+} ions.

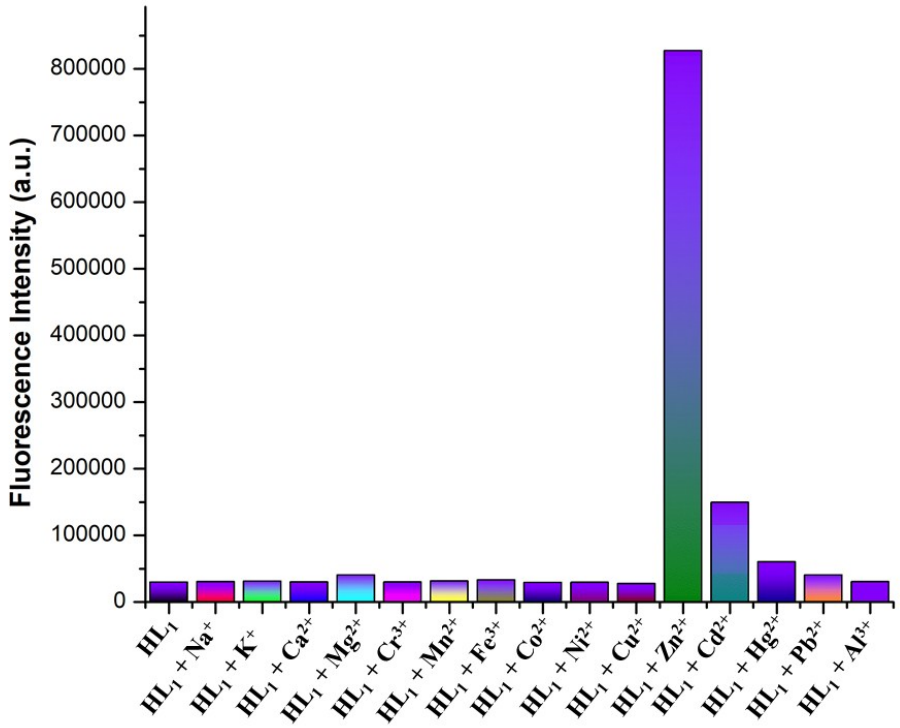

Fig. S25 Variation of fluorescence intensity of $\mathbf{HL_1}$ (10 μM) in presence of different common metal ions (5 μM) in 10 mM HEPES buffer solution at pH 7.4.

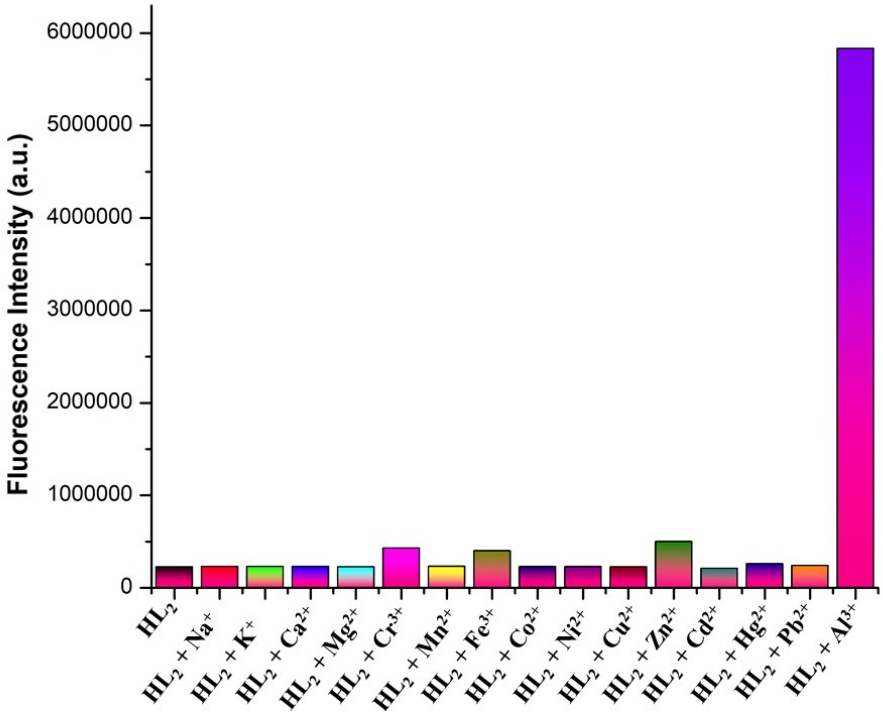

Fig. S26 Variation of fluorescence intensity of $\mathbf{HL_2}$ (10 μM) in presence of different common metal ions (5 μM) in 10 mM HEPES buffer solution at pH 7.4.

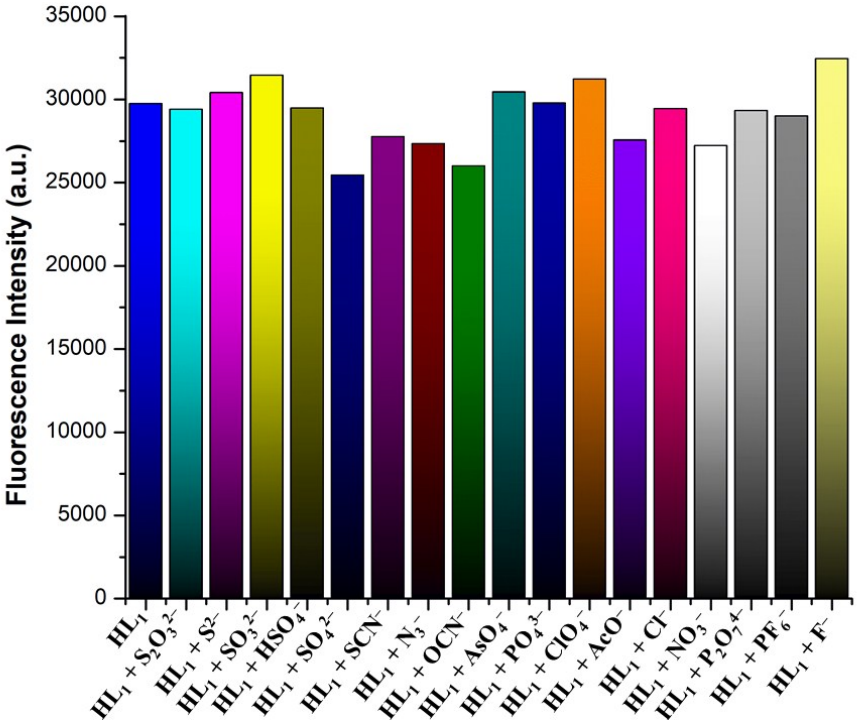

Fig. S27 Variation of fluorescence intensity of **HL_1** (10 μM) in presence of different common anions (5 μM) in 10 mM HEPES buffer solution at pH 7.4.

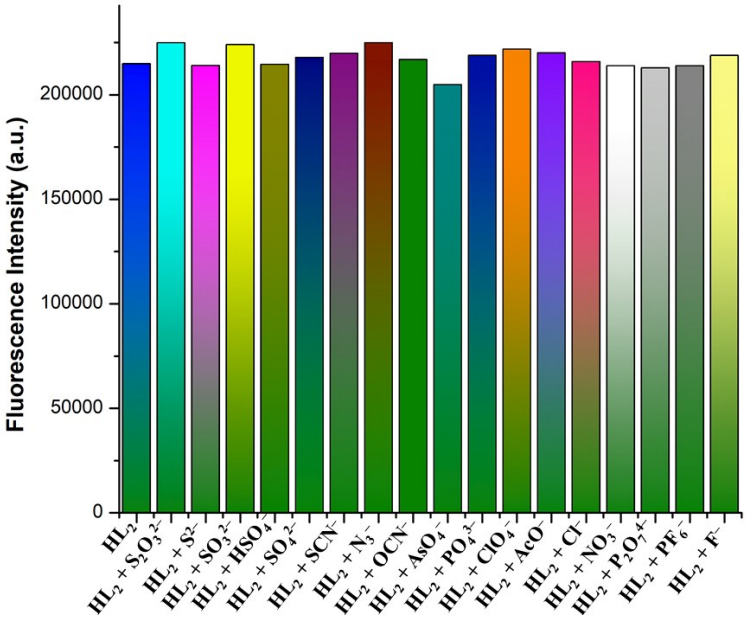

Fig. S28 Variation of fluorescence intensity of **HL_2** (10 μM) in presence of different common anions (5 μM) in 10 mM HEPES buffer solution at pH 7.4.

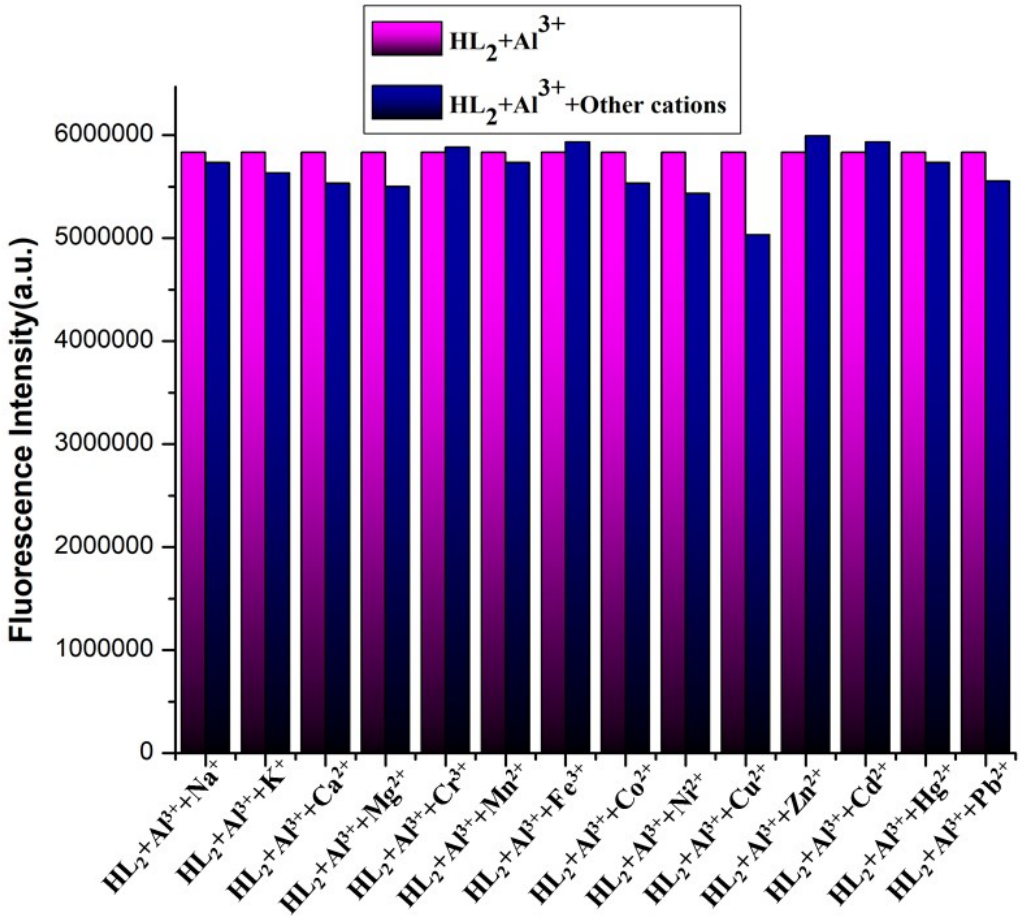

Fig. S29 Relative fluorescence intensity profile of [$(\mathbf{L_2})_2$–Al^{3+}] system in the presence of different common cations in 10 mM HEPES buffer at pH 7.4. Here, [$\mathbf{HL_2}$]= 10 μM; [Al^{3+}]= 5 μM; [other cations]= 50 μM.

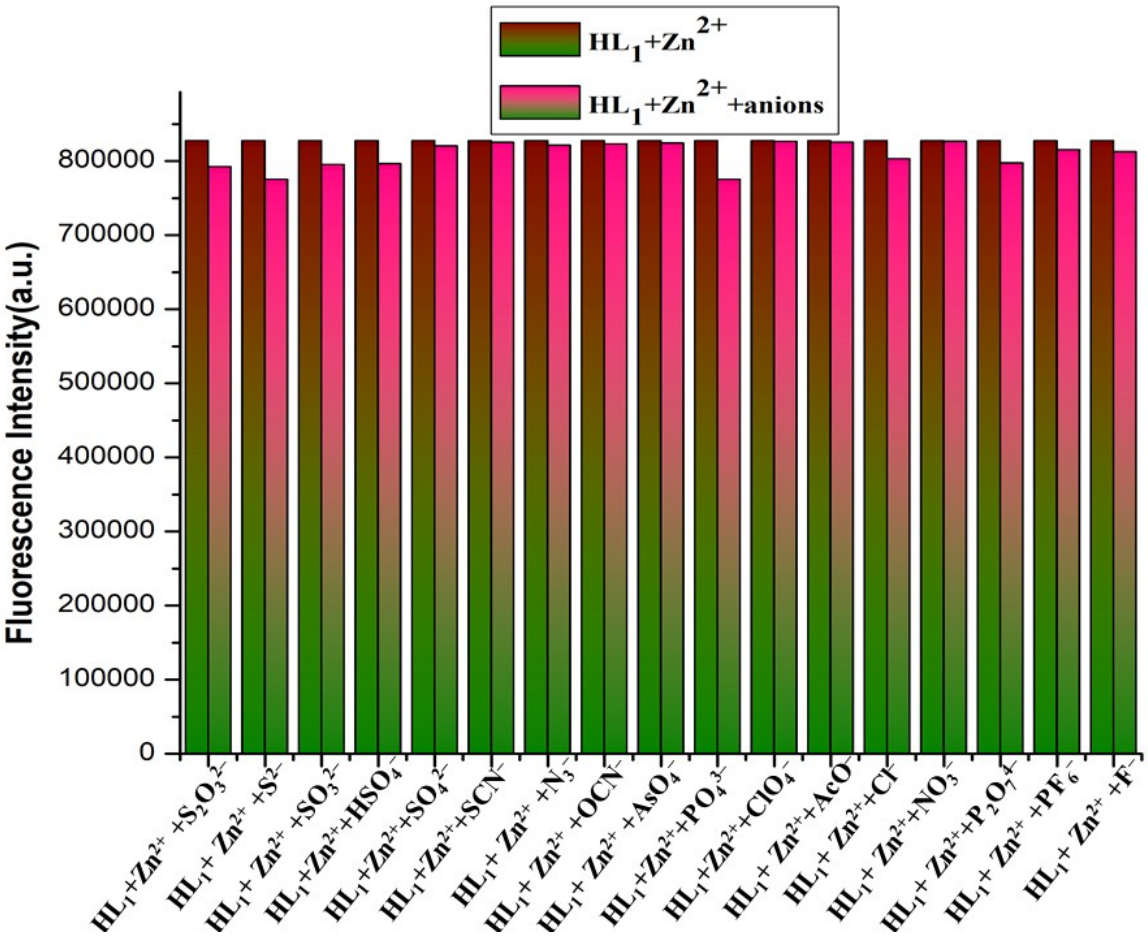

Fig. S30 Relative fluorescence intensity profile of [$(\mathbf{L_1})_2$–Zn^{2+}] system in the presence of different common anions in 10 mM HEPES buffer at pH 7.4. Here, [$\mathbf{HL_1}$] 10 μM; [Zn^{2+}]= 5 μM; [anions]= 50 μM.

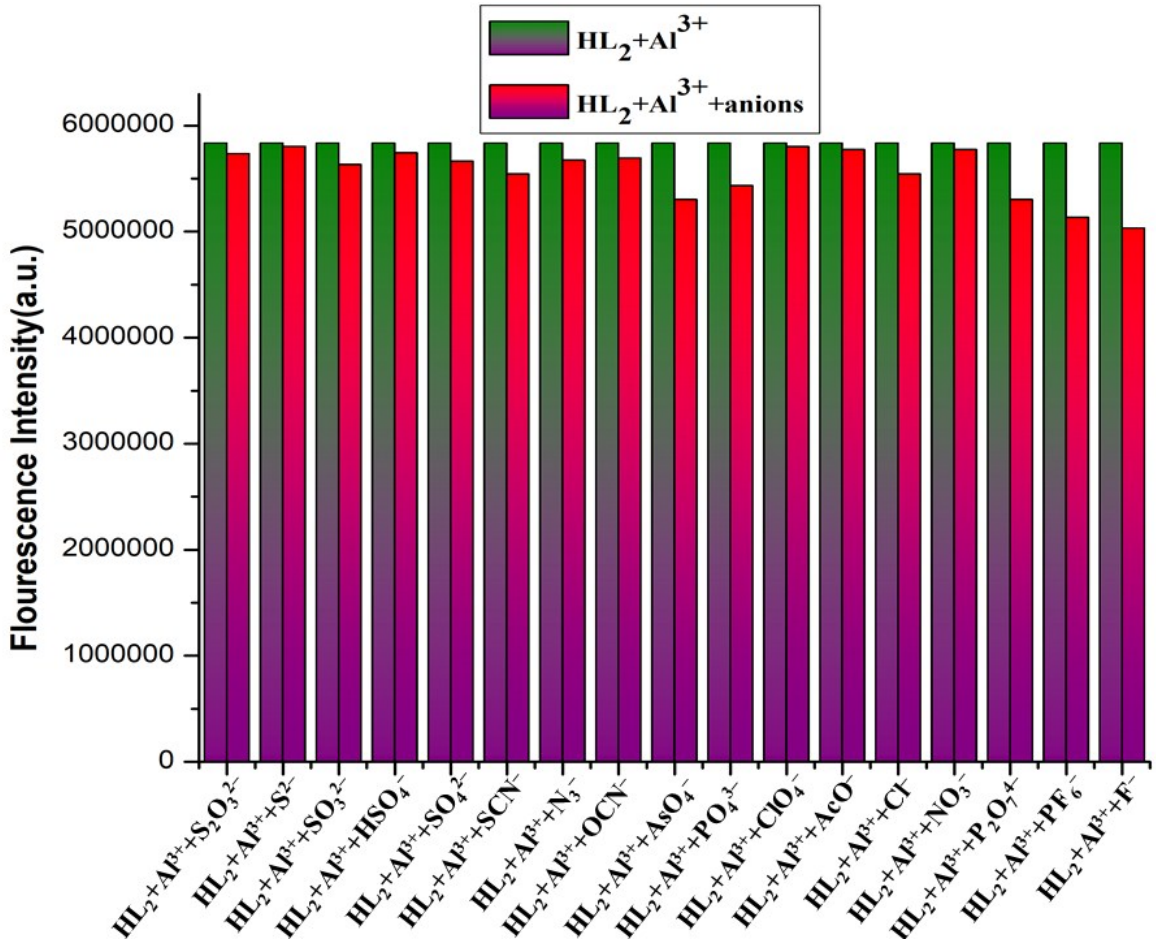

Fig. S31 Relative fluorescence intensity profile of [$(\mathbf{L_2})_2$–Al^{3+}] system in the presence of different common anions in 10 mM HEPES buffer at pH 7.4. Here, [$\mathbf{HL_2}$]= 10 μM; [Al^{3+}]= 5 μM; [anions]= 50 μM.

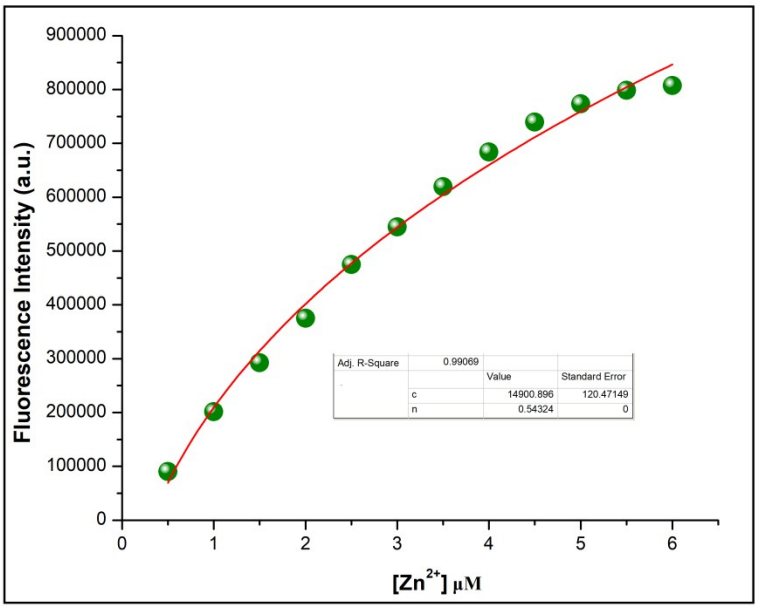

Fig. S32 Non-linear least square curve fitting for complex **1** by using fluorescence titration plot of $\mathbf{HL_1}$ in presence of Zn^{2+} ions.

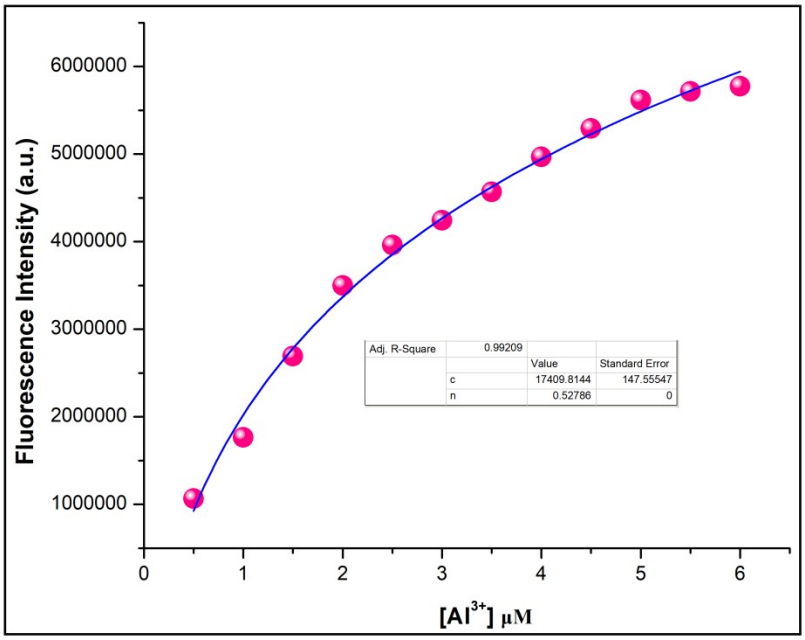

Fig. S33 Non-linear least square curve fitting for complex **2** by using fluorescence titration plot of $\mathbf{HL_2}$ in presence of Al^{3+} ions.

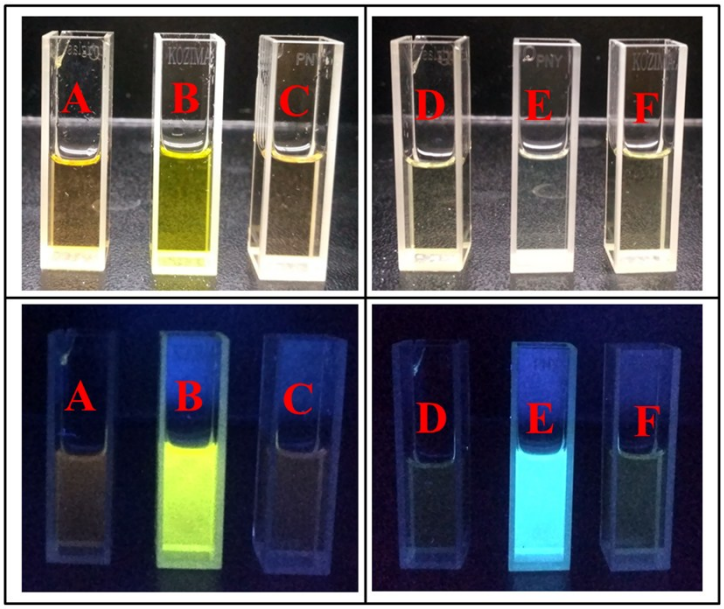

Fig. S34 Visual colour changes in reversibility experiments in 10mM HEPES buffer (pH 7.4) medium. Here, A= **HL_1** (10μM), B= **HL_1** (10μM) + Zn^{2+} (5 μM), C= **HL_1** (10μM) + Zn^{2+} (5 μM) + $EDTA^{2-}$ (5 μM), D= **HL_2** (10μM), E= **HL_2** (10μM) + Al^{3+} (5 μM) and F= **HL_2** (10μM) + Al^{3+} (5 μM) + $EDTA^{2-}$ (5 μM). Above images are taken under normal light and below images are taken under UV lamp.

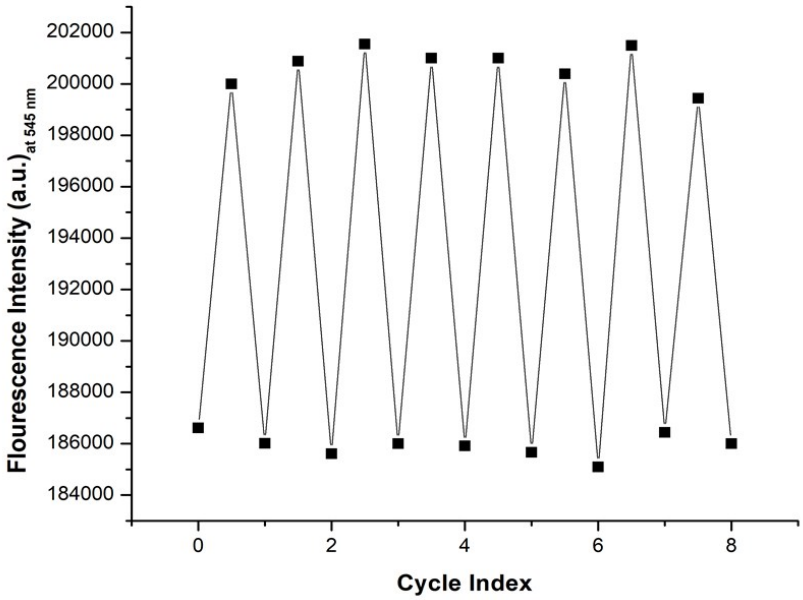

Fig. S35(a) Fluorescence reversibility experiment of **HL_1** between pH 4 and 10.

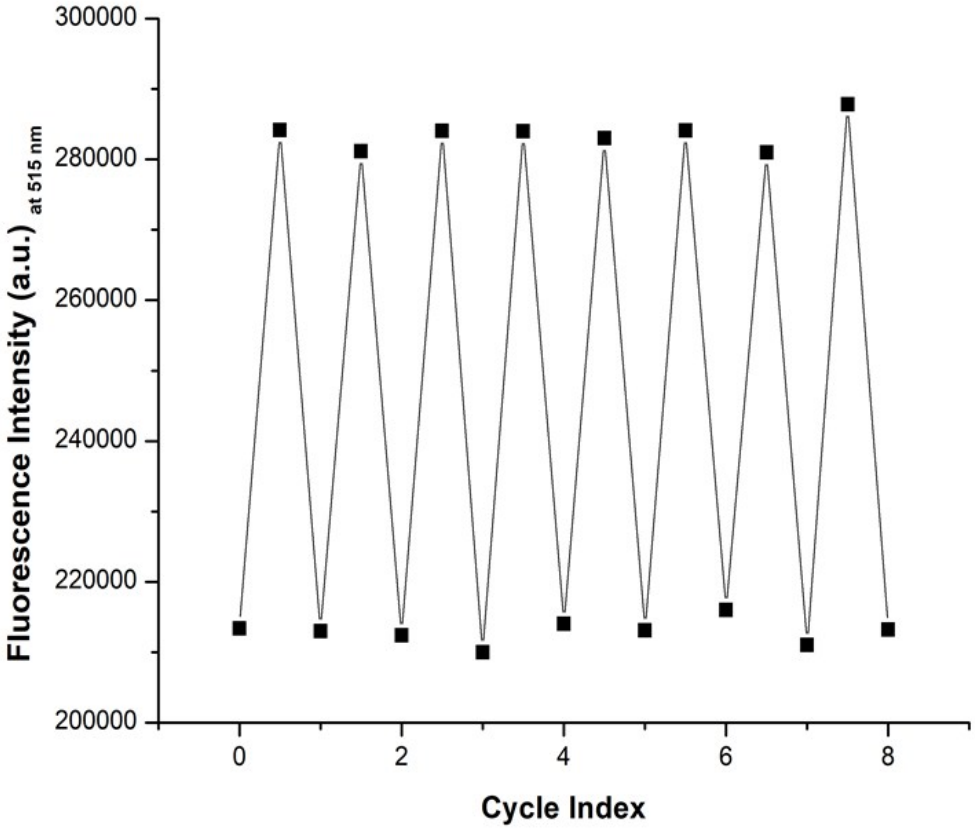

Fig. S35(b) Fluorescence reversibility experiment of **HL_2** between pH 4 and 10.

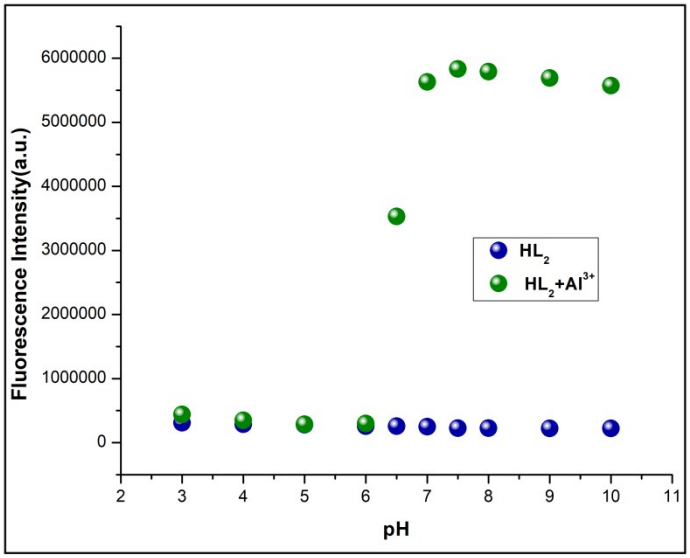

Fig. S36 Fluorescence intensity of **HL_2** (10 μM) in the absence and presence of Al^{3+} ions (5 μM) at various pH values in 10 mM HEPES buffer.

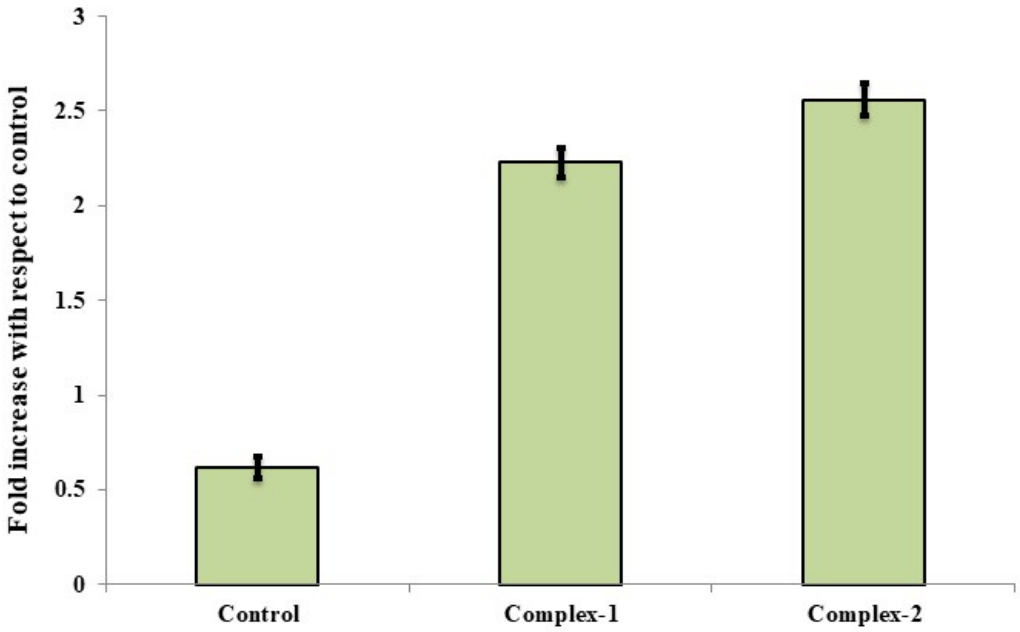

Fig. S37 Reactive oxygen species (ROS) generation using *MDA-MB 468* cell lines after 12h in presence of complexes **1** and **2**.

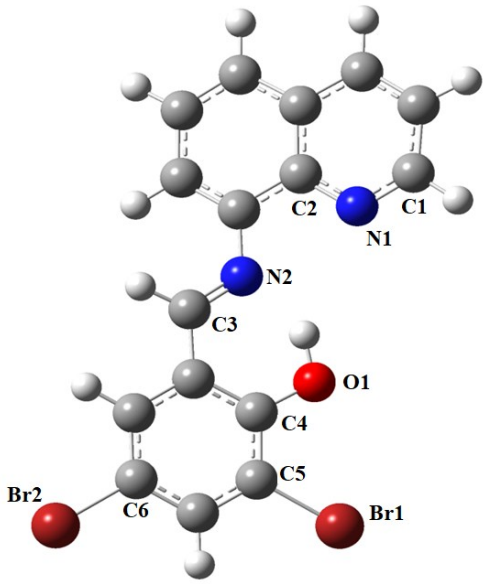

Fig. S38 DFT optimized structure of **HL$_1$**.

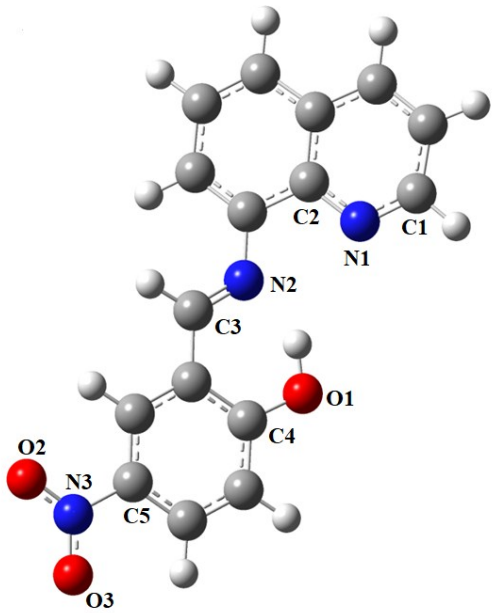

Fig. S39 DFT optimized structure of **HL$_2$**.

	HL_1	**HL_2**
LUMO+2	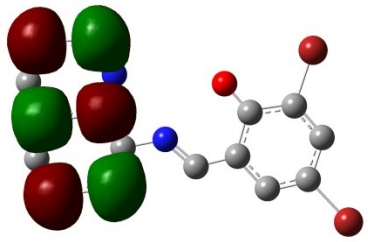	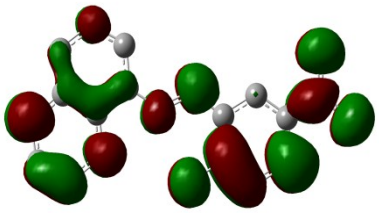
LUMO+1	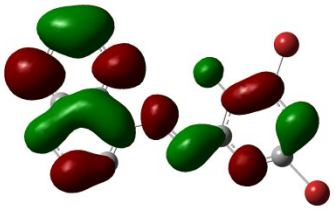	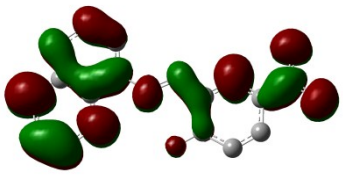
LUMO	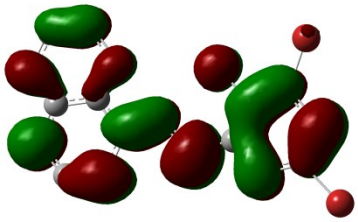	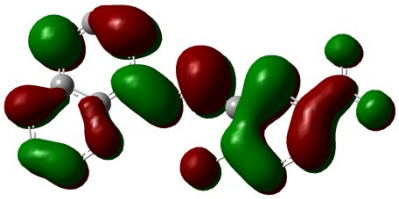
HOMO	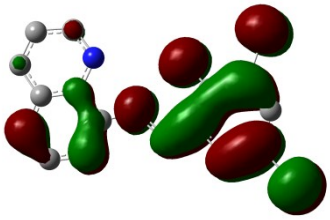	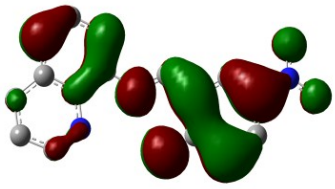
HOMO-1	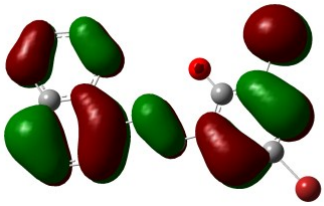	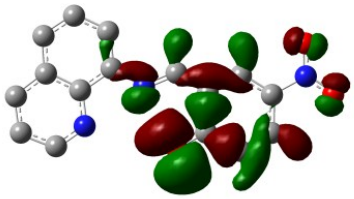
HOMO-2	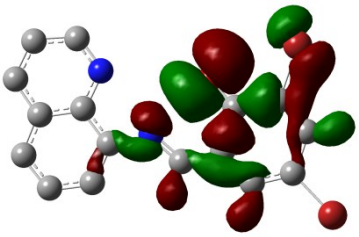	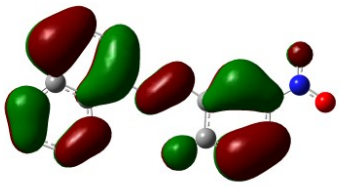

Fig. S40 Contour plots of some selected molecular orbital of $\mathbf{HL_1}$ and $\mathbf{HL_2}$.

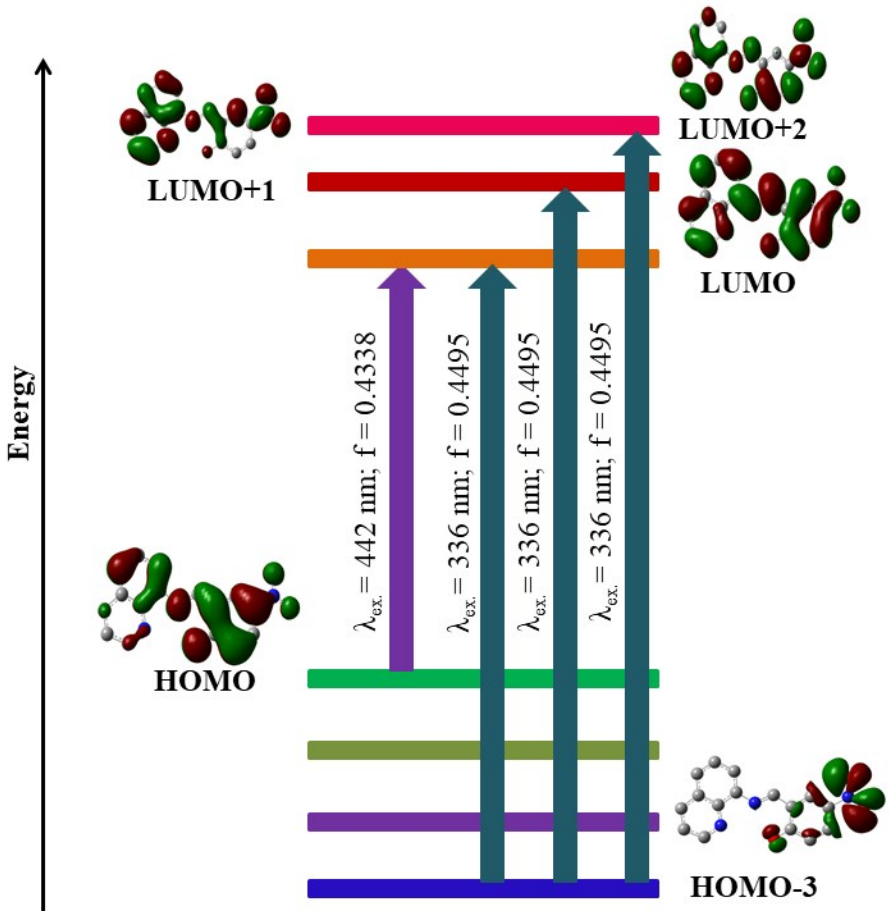

Fig. S41 Pictorial representation of key transitions of chemosensor $\mathbf{HL_2}$.

Table S1 Crystallographic parameters and refinement details of complexes **1** and **2**.

Complex	**1**	**2**
Empirical formula	$C_{33}H_{18.50}Br_4Cl_3N_4O_2Zn$	$C_{32}H_{20}AlN_7O_9$
Formula weight	994.38	673.53
Temperature (K)	273(2)	273(2)
Crystal system	triclinic	monoclinic
Space group	*P -1*	*P* $2_1/n$
a (Å)	11.5856(9)	12.5503(9)
b (Å)	12.9455(10)	14.1977(10)
c (Å)	13.6796(10)	16.8800(12)
α(°)	80.891(3)	90
β(°)	66.130(3)	101.622(2)
γ(°)	63.965(3)	90
Volume (Å^3)	1685.3(2)	2946.1(4)
Z	2	4
D_{calc} (g cm^{-3})	1.959	1.519
Absorption coefficient (mm^{-1})	5.747	0.141
F(000)	963	1384
θ Range for data collection (°)	1.751-27.202	1.89- 27.11
Reflections collected	52107	42415
Independent reflection / R_{int}	3548/0.2031	5168/ 0.0277
Data / restraints / parameters	7292/0/424	6465/0/ 450
Goodness-of-fit on F^2	1.159	1.510
Final *R* indices [I>2σ(I)]	R1 = 0.1150; wR2 = 0.1490	R1 = 0.0936; wR2 = 0.3187
R indices (all data)	R1 = 0.2214; wR2 = 0.1781	R1 = 0.1071; wR2 = 0.3438
Largest diff. peak / hole (e Å^{-3})	0.825/ -0.809	1.888/-0.590

Table S2 Binding constant and LOD values of complexes **1** and **2**.

	Binding constant (k) (M^{-1})		Limit of detection (LOD) (M)
	From UV-Vis study	From fluorometric study	
Complex **1**	$(1.33\pm0.04) \times 10^4$	$(1.49\pm0.01) \times 10^4$	1.39×10^{-7}
Complex **2**	$(1.65\pm0.008) \times 10^4$	$(1.74\pm0.01) \times 10^4$	1.50×10^{-7}

Table S3 Life time and quantum yield values of chemosensors and complexes **1** and **2**.

	Life time (ns)	χ^2	Quantum Yield (Φ)
HL_1	3.15	1.15	0.019
HL_2	1.45	1.02	0.054
Complex **1**	3.91	1.10	0.170
Complex **2**	1.50	0.98	0.210

Table S4 LD 50 values of complexes **1** and **2.**

Complex	***MDA-MB 468***	***SiHa***
1	88±2.8	86±2.7
2	92±2.3	95±1.8

Table S5 Energy (eV) of selected M.O.s of chemosensors (**HL_1** and **HL_2**).

	HL_1	**HL_2**
LUMO+5	0.35	0.56
LUMO+4	0.1	0.04
LUMO+3	-0.06	-1.08
LUMO+2	-0.94	-1.6
LUMO+1	-1.59	-1.8
LUMO	-2.51	-2.72
HOMO	-5.4	-5.83
HOMO-1	-6.4	-6.69
HOMO-2	-6.68	-6.72
HOMO-3	-7.08	-7.44
HOMO-4	-7.37	-7.53
HOMO-5	-7.39	-7.64

Table S6 Electronic transition calculated by TDDFT using B3LYP/CPCM method in methanol solvent of chemosensors (**HL_1** and **HL_2**).

	$E_{excitation}$ (ev)	$\lambda_{excitation}$ (nm)	Osc. Strength (f)	Key transition	Transition assigned
HL1	2.61	474	0.3115	HOMO $\rightarrow$ LUMO (99%)	n→π*
	3.50	353	0.3617	HOMO-1 $\rightarrow$ LUMO (93%)	π →π*
HL2	2.80	442	0.4338	HOMO $\rightarrow$ LUMO (99%)	n→π*
	3.68	336	0.4495	HOMO-3 $\rightarrow$ LUMO (48%) HOMO-3 $\rightarrow$ LUMO+1 (24%) HOMO-3 $\rightarrow$ LUMO+2 (16%)	π →π*

Chart S1 Previously reported quinoline based different chemosensing probes

Probe	Crystal Structure	Sensing of metal ion(s)	Excitation(nm)/ Emission(nm)	Sensing Media	Binding constant	Limit of detection (LOD)	Biological study	**Refs.**
HL	-	Al^{3+}, Zn^{2+} and F^{-}	416/500, 416/530, -	EtOH–H_2O solution (v/v = 4/1, 0.01 M, Tris-HCl buffer, pH = 7.30)	6.83×10^4 M^{-1}, 2.06×10^4 M^{-1} -	23.5 nM, 11.5 nM and 86.0 nM	Yes	**55a**
4-methyl-2-((quinolin-6-ylimino)methyl)phenol (6-QMP)	-	Al^{3+} and Zn^{2+}	415/543 and 415/525	10 mM HEPES buffer in water :methanol (1 : 9, v/v) (pH 7.4)	3.4×10^4 M^{-1}, 8.8×10^4 M^{-1}	23.4 nM and 53.7 nM	Yes	**55b**
4-methyl-2-((quinolin-2-ylimino)methyl)phenol (2-QMP)	-	Al^{3+} and Zn^{2+}	330/376 and 435/550	10 mM HEPES buffer in water :methanol (1 : 9, v/v) (pH 7.4)	3.86×10^4 M^{-1}, 8.18×10^4 M^{-1}	3.79 μM and 136.3 nM	Yes	**55b**
N-(quinoline-8-yl)pyridine-2-carboxamide (Hbpq)	Yes	Zn^{2+} and Co^{2+}	370/481 and 401/-	CH_3CN	7.0×10^{11} M^{-2} and 4.0×10^{11} M^{-2}	7.93×10^{-7} M and 2.20×10^{-6} M	Yes	**55c**
AQZ-2COOH	Yes	Zn^{2+}	350/510	Tris-HCl buffer	3.6×10^9 M^{-1}	0.10 μM	Yes	**55d**
2-amino-(quinolin-8-yl)acetamide (1)	Yes	Zn^{2+} and Cd^{2+}	300/504	Tris-HCl aqueous buffer pH 7.4 solution containing methanol (1% v/v) and Ethanol	1.41×10^6 M^{-1} and 8.45×10^6 M^{-1}	1.6 μM, -	Yes	**55e**
((E)-2-methoxy-N-((quinolin-2-yl)methylene)aniline) (MQA)	Yes	Zn^{2+} and Hg^{2+}	350/565 and 350/530	DMSO/water mixture (1/99 v/v)	1.52×10^4 M^{-1} and 1.41×10^5 M^{-1}	0.011 μM and 0.040 μM	-	**55f**
L_1	-	Zn^{2+} and $H_2PO_4^-$	390/525 and 390/430	DMSO/H_2O (v/v = 8 : 2)	1.94×10^4 M^{-1}, -	41.0 nM, -	Yes	**55g**
N-(quinoline-8-yl)pyrazine-2-carboxamide (Hqpzc)	-	Zn^{2+} and Cu^{2+}	360/476 and 378/-	acetonitrile	3.837×10^4 M^{-1} and 7.352×10^7 M^{-1}	1.11×10^{-6} M and 1.48×10^{-5} M	-	**55h**
1-((quinolin-3-ylimino)methyl)naphthalen-2-ol (HL)	-	Al^{3+} and F^{-}	350/464 and 350/412	methanol	7.784×10^8 M^{-1}	75.19 nM, -	-	**55i**

					-			
L2	-	Zn^{2+} and F^-	400/500 and 400/475	DMSO	-	2.1×10^{-7} M, -	-	**55j**
HL	-	Zn^{2+}	420/483	$MeOH/H_2O$ (4:1; pH=7.4)	1.69×10^4 M^{-1}	5.81×10^{-6} M	-	**55k**
L1	-	Zn^{2+}	360/500	H_2O/ethanol (8 : 2, v/v)	-	0.65 μM	Yes	**55l**
HAQT	Yes	Zn^{2+}	342/488	Tris buffer (pH = 7.40, $CH_3OH–H_2O$ = 4 : 1, v/v)	5.18×10^5 M^{-1}	2.56×10^{-7} M	-	**55m**
1	-	Zn^{2+}	350/536	10 mM bis-tris, pH 7.0	1.4×10^4 M^{-1}	4.48 μM	-	**55n**
2-methoxy-6-((quinolin-8-ylimino)methyl)phenol (HL)	Yes	Zn^{2+}	461/594	9:1 v/v $MeCN/H_2O$ in Tris–HCl buffer at pH 7.2	1.05×10^4 M^{-1}	1.3×10^{-7} M	Yes	**55o**
2,4-dichloro-6-(quinolin-8-ylimino)methyl)phenol (HL)	Yes	Zn^{2+}	454/553	1:1,v/v $CH_3CN:H_2O$ in HEPES buffer at pH = 7.2	3.10×10^5 M^{-2}	5.0×10^{-9} M	Yes	**55p**
BFQ	-	Zn^{2+}, Al^{3+} and F^-	395/560, 395/530 and 420/610	EtOH–H2O(v/v =9/1) and MeCN	$(8.51\pm0.25)\times10^{10}$ M^{-2}, $(1.53\pm0.18)\times10^{10}$ M^{-2} and $(8.37\pm0.17\times10^8$ M^{-2}	$(3.56\pm0.14)\times10^{-6}$ M, $(1.14\pm0.11)\times10^{-6}$ M and $(3.68\pm0.21)\times10^{-6}$ M	-	**55q**
2,4-Dibromo-6-((quinolin-8-ylimino)methyl)phenol (HL_1)	Yes	Zn^{2+}	440/540	10 mM HEPES buffer at pH 7.4	$(1.33\pm0.04)\times10^4$ M^{-1}	1.39×10^{-7} M	Yes	**This work**
4-Nitro-2-((quinolin-8-ylimino)methyl)phenol) (HL_2)	Yes	Al^{3+}	400/475	10 mM HEPES buffer at pH 7.4	$(1.65\pm0.008)\times10^4$ M^{-1}	1.50×10^{-7} M	Yes	**This work**